



Microplankton Interactions with Decadal-Scale Nutrient Enrichment in a Deep Estuary, with Implications for Eutrophication—Related Ecosystem Stressors

Karl Safi¹ · John Zeldis² · Leigh Tait² · Karen Robinson² · Mark Gall³ · Karen Thompson¹

Received: 2 May 2021 / Revised: 7 June 2022 / Accepted: 7 June 2022 / Published online: 7 July 2022
© The Author(s) 2022

Abstract

Long-term (decadal) records of microplankton provide insights into how lower trophic levels of coastal ecosystems respond to nutrient enrichment, over and above shorter-term variability. We used a 15-year seasonal census in the Firth of Thames, a deep, nutrient-enriched estuary in northeastern Aotearoa/New Zealand, to determine microplankton responses to enrichment. Kendall trend analyses showed that dissolved inorganic nitrogen (DIN) and dissolved organic nitrogen were enriched by 99% and 34%, respectively, over 15 years, while phosphorus changed little. Larger phytoplankton ($> 2 \mu\text{m}$) increased by 46%, including 57% increases by diatoms (mainly large centrics with 93% increase) and nanoflagellates (151% increase). Dinoflagellates decreased by 46%, such that the community shifted from dinoflagellate to diatom/nanoflagellate dominance. Within phytoplankton $\leq 2 \mu\text{m}$, picoprokaryotes increased by 369%, while picoeukaryotes changed little. Among microheterotrophs ($< 200 \mu\text{m}$), bacteria increased by 89%, and small oligotrichs increased by 53%. Trend analyses and multivariate general additive modelling showed that microplankton biomass responded primarily to increased DIN over the 15-year period and secondarily to stratification variation at shorter time scales. The changed biomasses and community composition are explained as responses to increased N:P and food-web interactions. Deleterious changes included increased toxic *Pseudo-nitzschia* abundance and potentially reduced nutritional quality of the phytoplankton community for grazers. The increased N and larger diatoms indicated potential for increased deposition to sediments, possibly explaining previous observations of lowered denitrification in the Firth during the time series period. The results indicated a continuation of enrichment the Firth has received over decades, with implications for expression of ecosystem stressors of acidification and hypoxia.

Keywords Phytoplankton time series · Trend analysis · Plankton food webs · Coastal eutrophication · Denitrification · Coastal acidification

Introduction

Coastal ecosystems are threatened by stressors arising from nutrient enrichment and eutrophication (Alexander et al. 2017; Rabalais et al. 2009), including depleted oxygen (O_2),

lowered pH (Conley et al. 2009; Gobler et al. 2014; Paerl 2006), and changed phytoplankton biodiversity including increases in harmful algae (Capriulo et al. 2002; Sutula 2011). While it is well-known that auto- and heterotrophic microplankton ($< 200 \mu\text{m}$) are pivotal in mediating water column biogeochemical cycles (Falkowski et al. 1992), less well-understood is how changing microplankton biomass, taxonomic structure, and diversity interacts in expression of these biogeochemical stressors (NRC 2000). When conducted in tandem with biogeochemical studies, long-term (decadal-scale) studies of marine plankton communities can provide useful insights into how lower trophic levels of coastal ecosystems respond to nutrient enrichment and are involved in the expression of eutrophication-related stressors (Eriksen et al. 2019; Kemp et al. 2005; NRC 2000; Philippart et al. 2000).

Communicated by James L. Pinckney

✉ Karl Safi
karl.safi@niwa.co.nz

¹ National Institute of Water and Atmospheric Research, P.O. Box 11-115, Hamilton, New Zealand

² National Institute of Water and Atmospheric Research, PO Box 8602, Christchurch, New Zealand

³ National Institute of Water and Atmospheric Research, Private Bag 14901, Wellington, New Zealand

The degree to which primary production is exported and mineralised, as well as its cycling within the microbial loop, affects its role in mediating eutrophication-related stressors (Capriulo et al. 2002). Nutrient enrichment can be expected to promote larger-celled phytoplankton, by relieving nutrient limitation in large cells that have small surface-to-volume ratios (Chisholm 1992). Cooper (1995) and Ragueneau et al. (1994) described increases in ratios of large centric diatoms relative to smaller pennate diatoms during early phases of eutrophication of Chesapeake Bay (Kemp et al. 2005). Philippart et al. (2000) showed that enrichment-driven increases in large cells can lead to accentuated vertical export upon seasonal nutrient limitation and senescence, when cells settle to depth and are mineralised. Enrichment effects on taxonomic structure thus have implications for vertical biomass distribution and export toward mineralisation pathways. Also, as biomass increases due to enrichment, so may the incidence of harmful algal bloom species (Anderson et al. 2008; Cloern 2001) with the potential for associated deleterious ecological effects.

Microheterotrophic (< 200 µm) communities (bacteria, small heterotrophic flagellates and microzooplankton) respond quickly to enrichment of autotrophic populations (Azam et al. 1983; Krstulović et al. 1998). Bacteria drive mineralisation pathways and production of dissolved organic matter originating in large part from phytoplankton, which in turn can support small heterotrophic and mixotrophic flagellates (Antia et al. 1991; Flynn et al. 2019). Microzooplankton grazers adapt quickly to changing bacterial and phytoplankton populations, with the sizes of microzooplankton grazers directly linked to the size of their prey (Hansen et al. 1994). We would therefore expect changes in enrichment and autotrophic population structure to be reflected in microheterotrophs, which will contribute to the respiratory metabolism of the water column, and hence potential for reduced O₂, increased CO₂ and acidification (Shen et al. 2019; Sunda and Cai 2012; Wallace et al. 2014; Zhou et al. 2020). Concomitant assessment of both autotrophic and heterotrophic components will thus improve understanding of ecosystem responses to enrichment at the base of the food web, with implications for potential ecological stressors.

In this study, we describe decadal-scale changes in the autotrophic and heterotrophic plankton in the Firth of Thames, in northern Aotearoa/New Zealand (NZ), over 15 years (1998–2013). The Firth is a large (1100 km², 15 m average depth), drowned-valley estuary (Hume et al. 2016) that opens to the Hauraki Gulf (Fig. 1). It supports some of NZ's largest marine farms (for mussels) and is an important region for recruitment to its largest inshore fin-fishery (for snapper) (Kelly et al. 2020; Peart 2016; Zeldis and Francis 1998). Total nitrogen (TN) loading to the Firth, primarily from the Waihou and Piako rivers at its head (Fig. 1B), has increased substantially above natural levels (by ~82%:

Snelder et al. 2018). The agricultural intensification driving this loading increase is historical, having occurred over many decades, commencing in the early 1900s with drainage of wetlands and peat swamps, but undergoing rapid expansion in the 1980s and 1990s primarily for dairy farming (Judd 2015; Kelly et al. 2020; Peart 2016). Currently, about 78% of TN runoff to the Firth is anthropogenic (Vant 2013), and catchment runoff now dominates its nutrient loading, with ~85% of its dissolved inorganic nitrogen (DIN) supply arising from its catchment (Zeldis and Swaney 2018). As a consequence, the Firth now sustains volumetric primary production roughly double that of the seaward Hauraki Gulf (Gall and Zeldis 2011; Zeldis et al. 2022; Zeldis and Willis 2015). It has a pronounced seasonal cycle of net ecosystem metabolism that evolves from net autotrophy in spring and early summer to net heterotrophy from late summer through autumn, when it often expresses significantly depressed pH and hypoxia (Law et al. 2019; Zeldis et al. 2022; Zeldis and Swaney 2018).

Nutrient enrichment of the Firth has continued during the more recent period of the present study (1998–2013), with increases in DIN and dissolved organic nitrogen (DON) concentrations (Zeldis and Swaney 2018). To investigate how microplankton at the base of the Firth food web have responded to nutrient enrichment, here we describe decadal-scale changes in its phytoplankton and microheterotrophic biomasses and diversity. We place these changes into ecological context by assessing the inter-annual and seasonal dynamics of the microplankton taxonomic groups, their responses to the changed nutrient environment and trophic interactions. We assess potential causes of the N increases the Firth has received over the recent period and the role of microplankton in that enrichment. We conclude by describing the roles of microplankton in the expression of pH and O₂-related stressors currently seen in the Firth.

Methods

Sampling of Nutrients, Physical Properties, Phytoplankton, Bacteria and Microzooplankton

Surveys were conducted at the NIWA (National Institute of Water and Atmospheric Research, New Zealand) Firth of Thames monitoring site (Fig. 1B) during 57 voyages made at seasonal (quarterly) intervals from September 1998 to December 2013. Sampling was typically in austral spring (September/October), summer (December), autumn (March) and winter (July), except for July 2001 to December 2002, when sampling was not conducted. Physical samples were acquired from September 1998 to December 2013 using a conductivity–temperature–depth (CTD: Seabird 911*plus*) instrument, fitted with O₂ and water transmissivity sensors

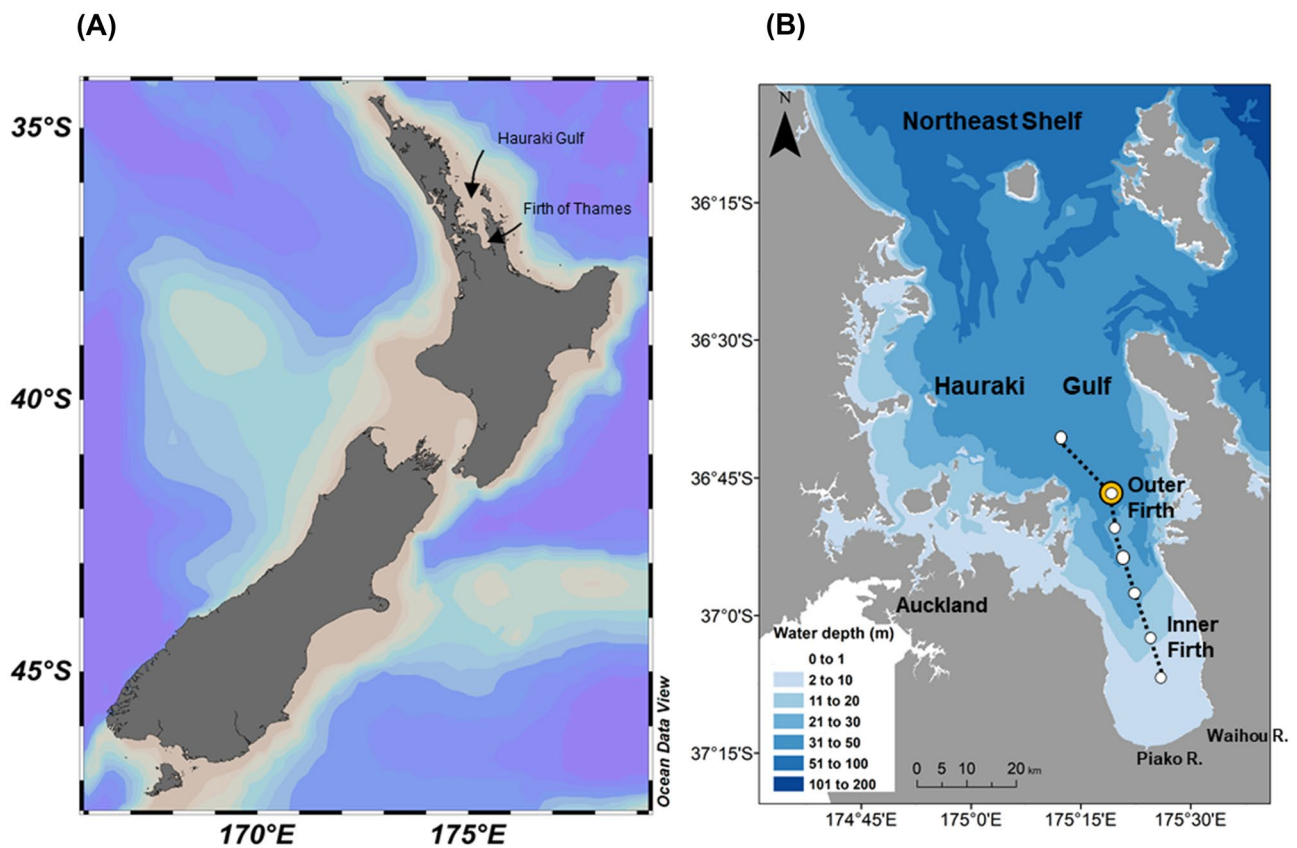


Fig. 1 **A** Hauraki Gulf and Firth of Thames in northern Aotearoa/New Zealand. **B** Hauraki Gulf and Firth of Thames showing bathymetry, location of Auckland City and major River mouths (Waihou and

Piako rivers) entering the Firth. The orange circle marks the Firth monitoring site. The open circles mark the transect of sampling stations plotted in Fig. 9

and a water sampling rosette fitted with 10-L Niskin bottles, deployed from the RVs *Kaharoa* (28 m), *Tangaroa* (78 m) or *Star Keys* (19 m). Physical samples were resolved at 1 m depth intervals through the 40 m water column. CTD sensors were factory calibrated within the interval recommended by the manufacturer (2 years) and had accuracies of 0.002 °C, 0.003 mS/cm and 2% of surface O₂ saturation, respectively. Transmissivity was sampled using a Seabird C-Star transmissometer (25 cm path length).

Additional seasonal surveys were conducted on a station transect through the Firth and into the Hauraki Gulf (Fig. 1B) in spring, summer, autumn and winter 2012–2013 and autumn 2010, as part of research in the wider Hauraki Gulf/Firth region that examined its carbonate and O₂ environments (Zeldis et al. 2022). These surveys used CTD-rosette sampling and analysis protocols identical to those at the Firth monitoring site.

Water samples were collected at the monitoring site using the rosette at 6 depths, typically 3–5 m, 9–11 m, 13–16 m, 20–23 m, 28–31 m and 33–38 m, depending on tide and sea state that affected ship movement. Dissolved macronutrients and phytoplankton pigments (chlorophyll *a* (chl-*a*),

phaeopigment-*a* (phaeo-*a*)) were acquired from September 1998 to December 2013. Pigments were filtered using 250-mL Whatman GFF filters at <5 mm Hg pressure, with filtrate collected into acid-washed bottles for dissolved macronutrients (both immediately frozen on board at –20° C). In the lab, frozen filters for chl-*a*/phaeo-*a* were defrosted, extracted in 90% ice cold acetone overnight in the dark (refrigerated) and the extract read against a chl-*a* standard using spectrofluorometry (Varian Cary Eclipse Fluorometer) following the APHA 10200 H (Baird 2017) method. Extracts were then acidified and re-read to obtain phaeo-*a* concentrations (detection limit 0.01 µg L⁻¹ for both chl-*a* and phaeo-*a*). Nutrient samples were thawed and assayed using flow injection analysis for seawater on an Astoria Pacific (API 300) microsegmented flow analyser with digital detector for nitrate (NO₃⁻-N) and ammonium (NH₄⁺-N: API methods 305-A177 and 305-A026, respectively), dissolved inorganic phosphorus (DIP: API Method 305-A204) and dissolved reactive silicate (DRSi: API method 305-A221) (Lachat 2010). Dissolved organic N (DON) was determined by differencing total dissolved nitrogen (TDN: method 10-107-04-3-B (Lachat 2010)) with the sum of NO₃⁻-N and NH₄⁺-N (dissolved

inorganic nitrogen (DIN)). Dissolved organic phosphorus (DOP) was determined by differencing total dissolved phosphorus (TDP: API Methods 305-A204) (Lachat 2010), with DIP. Detection limits on these assays were $0.07 \mu\text{mol L}^{-1}$ for NO_3^- -N and NH_4^+ -N, $0.7 \mu\text{mol L}^{-1}$ for TDN, $0.03 \mu\text{mol L}^{-1}$ for DIP and TDP and $0.04 \mu\text{mol L}^{-1}$ for DRSi.

Samples (250 mL) for phytoplankton ($> 2 \mu\text{m}$ in size) and microzooplankton ($< 200 \mu\text{m}$) were acquired from September 1998 to July 2013. Samples were preserved in Lugol's iodine (1% final concentration) on board the vessel. In the lab, 50–250 mL sub-samples were settled in measuring cylinders with settling times of 0.5 h per millimetre of settling column depth. The supernatant was then siphoned off, and the remaining 10 mL was transferred to Utermohl chambers and resettled. Phytoplankton $> 2 \mu\text{m}$ were then enumerated using a Leica DMI3000B inverted microscope at $\times 100$ to $\times 600$ magnification (Edler and Elbrächter 2010). The cell-size lower detection limit for these microscope counts was $\sim 2 \mu\text{m}$. Samples were counted as soon as practicable after collection. Although samples were occasionally held for longer durations (up to months), there was no trend in how long they were held before analysis, within the ~ 15 -year time series. All abundant phytoplankton $> 2 \mu\text{m}$ at concentrations > 100 cells per L were identified to genus or species level where possible, counted and assigned to algal groups including diatoms (centric and pennate) and dinoflagellates (naked and armoured). Known toxin-producing species of dinoflagellates and diatoms were itemised into additional subgroups. Small flagellated cells (excluding dinoflagellates) were enumerated as nanoflagellates (most $< 20 \mu\text{m}$), including unspicied, Prymnesiophytes, Cryptophytes, Chrysophytes, unidentified monads and rarer populations of identified silicoflagellates, Raphidophytes and euglenoids. Heterotrophic and mixotrophic nanoflagellates were not separated from autotrophic nanoflagellates, and their populations were assessed as an undifferentiated group. All phytoplankton $> 2 \mu\text{m}$ sample analyses were conducted by the first author. Any changes in nomenclature were retrospectively applied to older data to keep systematics consistent. Acidified Lugol's iodine used for preservation of phytoplankton $> 2 \mu\text{m}$ was likely to have eliminated any calcium-based algae (coccoliths). However, subsequent counts with alkaline Lugol's iodine showed this group was not an important component of biomass in these waters.

Microzooplankton, including ciliates and larval copepods (nauplii), were determined from the same bulk Lugol's iodine samples as phytoplankton $> 2 \mu\text{m}$. Samples were analysed following similar protocols to phytoplankton, but settled volumes were 250 mL with supernatant siphoned and the remaining ~ 20 mL then transferred to Utermohl chambers and resettled (Edler and Elbrächter 2010). A wild inverted microscope was used for enumeration during 1998–2001 and then subsequently a Leitz Fluovert FS inverted microscope.

Microzooplankton were identified to genus where possible but with no differentiation of plastidic ciliates. All microzooplankton analyses were conducted by the fourth author.

Picophytoplankton (phytoplankton $\leq 2 \mu\text{m}$) and bacteria were sampled between December 2002 and December 2013 and frozen immediately on board in liquid N_2 in 1.8-mL cryovials (in triplicate). In the lab, samples were stored at -80°C and were thawed immediately before counting on a FACSCalibur 15 mW air-cooled argon-ion laser flow cytometer (fixed at 488 nm: Becton Dickinson, Mountain View, CA, USA) with CellQuest Vers. 3.3 software. Counts for picoprokaryotes (*Synechococcus*), picoeukaryotes and bacteria (stained) followed the methods of Hall et al. (2006). All flow cytometric samples were analysed by the sixth author within 2–3 months of collection.

Phytoplankton $> 2 \mu\text{m}$ biovolume estimates were calculated from the dimensions of each taxon using approximated geometric shapes (spheres, cones, ellipsoids), initially following Hillebrand et al. (1999) with some modifications following Sun and Liu (2003) and Olenina et al. (2006). Any changes in shape estimates for taxa were applied retrospectively, to avoid bias in estimates with time. Size categories within taxa were also used to reduce bias (e.g. 'small *Gyrodinium*' and 'large *Gyrodinium*'). The biovolumes were used to calculate cell carbon (mg C m^{-3}) using equations from Montagnes and Franklin (2001) for diatoms and Strathman (1967), Menden-Deuer and Lessard (2000) and Putt and Stoecker (1989) for dinoflagellates and nanoflagellates.

Ciliate cell C was estimated from dimensions of 10–20 randomly chosen individuals of each taxon using approximate geometric shapes and then converted to C biomass using a factor of $0.19 \text{ pg C } \mu\text{m}^{-3}$ (Putt and Stoecker 1989). Copepod naupliar cell C was estimated using a conversion factor of $0.032 \mu\text{g C individual}^{-1}$ (Uye and Sano 1998). Cell C biomasses for picoeukaryotes ($1319 \text{ fg C cell}^{-1}$) and picoprokaryotes ($154 \text{ fg C cell}^{-1}$) were estimated following Buitenhuis et al. (2012). Bacteria C biomass was estimated following Fukuda et al. (1998) using $30.2 \text{ fg C cell}^{-1}$.

Data Analysis

Data for physical parameters, nutrients and biological groups were depth-integrated using:

$$I = \frac{\sum_{i=1}^{n-1} \Delta Z_{i,i+1} 0.5(B_i + B_{i+1})}{\sum_{i=1}^{n-1} \Delta Z_{i,i+1}}$$

where I denotes a sample level number (incrementing from 1 at the sea surface), B_i denotes physical values or concentrations (depending on variate type) at sample level I and $\Delta Z_{i,i+1}$ is the thickness (m) of the layer between sequential

sampling depths. In analyses where data were grouped by seasons, seasons were defined as September to November, December to February, March to May and June to August, for austral spring, summer, autumn and winter, respectively. Interpolated displays of data were visualised using Ocean Data View software (Schlitzer 2013).

Time-series temporal trends were assessed using non-parametric seasonal Kendall trend tests using ‘Time Trends’ software (Jowett 2019) with trend slope directions tested at $p=0.05$. Interpretation of the trends at that level considers the following precepts from McBride (2019) and Jowett (2019): (1) if the sign of both the upper and lower 90% (one-sided) confidence limits for the time trend (Sen) slope are the same (or one limit is zero), then it can be inferred that there is a trend at Kendall $p=0.05$, and (2) while the Kendall p value for significance of slope indicates the strength of trends, p values ≥ 0.05 are not sufficient evidence to suggest that no trend exists, but only that the null hypothesis (i.e. there is no trend) is ‘not rejected’ (McBride 2019). To accommodate this, and following McBride (2019) and Jowett (2019), the probability that the slope is truly below or above zero is calculated and further assessed for likelihood using the terms in Table 1 (Jowett 2019; Mastrandrea et al. 2010). Full trend statistics are given in the Supplementary Material Tables S1–S4 of this paper.

To assess changes of nutrient and microplankton values from the start to end of their respective time series, their median values (V) at the start and end were evaluated using:

$$V_{\text{start}} = V_M - S * \frac{L}{2} \text{ and } V_{\text{end}} = V_M + S * \frac{L}{2},$$

where V_M is the median value at the time series mid-point, S is the Sen slope of the Kendall seasonal trend standardised to a year and expressed in the units of the variable (Jowett 2019) and L is the time series length (y). Percentage changes from start to end of the respective time series were expressed as $(V_{\text{end}} - V_{\text{start}}) / V_{\text{start}} * 100$ and presented for values that had ‘increasing/decreasing trend possible’ or stronger. Time

series lengths were taken as 15.5 years for nutrients and pigments, 15.0 years for phytoplankton $> 2 \mu\text{m}$ and microzooplankton and 11.25 years for picophytoplankton and bacteria, based on their respective start and end dates (‘Sampling of Nutrients, Physical Properties, Phytoplankton, Bacteria and Microzooplankton’ section).











Associations between depth-integrated physical and nutrient predictors and phytoplankton and bacteria biomasses (i.e. the broad taxonomic groups: diatoms, dinoflagellates, nanoflagellates, picoprokaryotes, picoeukaryotes, oligotrichs, tintinnids, nauplii and bacteria) were assessed with multivariate General Additive Models (GAMs), using the package ‘mgcv’ (Wood 2006, 2011). GAMs were used to assess the potential for linear and non-linear covariance between continuous physical (temperature, salinity, stratification) and nutrient (DIN, DON, DIP) predictors and the categorical predictors ‘group’ (diatoms, dinoflagellates, nanoflagellates, picoprokaryotes, picoeukaryotes, oligotrichs, tintinnids, nauplii and bacteria) and ‘season’ (spring, summer, autumn, winter). Assumptions of normality (Q-Q plot) and homogeneity of variance (Levene’s test), as well as ‘concurvity’ for general additive model analysis (an estimate of redundancy among explanatory variables), were checked for the multivariate model. GAM models were fitted with ‘cr’ (cubic regression) splines, using a k -value of 10 (i.e. the number of ‘knots’ denoting the complexity of the non-linear fit), and the distribution family ‘tweedie’. Selection procedures were implemented to penalise and remove factors with poor explanatory power.

Results

Dissolved Nutrient Trends

Concentrations of DIN plotted by depth and time over the 15-year time series at the Firth monitoring site showed that the upper water column ($< 20 \text{ m}$) sustained persistently

Table 1 Assessments of strength of Kendall p value, associated confidence limits, slope direction probabilities and likelihood assessment terms (Jowett 2019; Mastrandrea et al. 2010; McBride 2019).

Kendall p	Confidence limits (%)	Slope direction probability	Likelihood categories	Symbol for category	
				Increase	Decrease
0.01	99	≥ 0.995	Virtually certain		
0.05	95	≥ 0.975	Very likely		
0.10	90	≥ 0.95	Likely		
0.33	67	≥ 0.835	Possible		
0.67	33	≥ 0.665	About as likely as not		
0.90	10	≥ 0.55	Unlikely		
0.95	5	≥ 0.525	Extremely unlikely		
0.99	1	≤ 0.505	Exceptionally unlikely		

Arrow symbols for trend directions and corresponding likelihood categories (used in Results) are shown, for cases where likelihoods were ‘About as likely as not’ or greater

depleted DIN median concentrations ($\sim 0.5 \text{ mmol m}^{-3}$), especially from spring through autumn, with higher concentrations below 20 m (Fig. 2). These DIN differences with respect to depth corresponded with observations by Zeldis and Swaney (2018) who showed (their Fig. 9) that the Firth pycnocline typically formed around 20 m depth, about mid-depth in the 40 m water column, separating the water column into a deeper layer (lower, $\geq 20 \text{ m}$) isolated from the upper layer (upper, $< 20 \text{ m}$) by density discontinuity. DIP also was often depleted in the upper water column (Fig. 2) but less so than DIN. Overall, DIN:DIP was low, with median values < 3.5 , well below the typical 16:1 Redfield ratio for N and P balanced growth (Redfield et al. 1963), indicating strong N-limitation of phytoplankton growth.

Seasonal Kendall trend tests (Fig. 3) showed that water column-integrated DIN had a ‘very likely’ increase of $4.3\% \text{ year}^{-1}$ (Table S1A), with increases of $4.1\% \text{ year}^{-1}$ and $4.4\% \text{ year}^{-1}$ in the lower and upper water columns, respectively (‘likely’ and ‘very likely’ trends) (Table S1B). Analysis by season showed that the season with the highest likelihood of an increasing DIN trend was summer ($6.0\% \text{ year}^{-1}$; Fig. 3; Table S1C). The $\text{NH}_4^+\text{-N}$ component of DIN had ‘likely increasing’ trend in the upper water column. DON was abundant relative to DIN (Table S1A) and had ‘very likely’ increase at $1.9\% \text{ year}^{-1}$, with the highest likelihood of increasing trend in autumn ($2.3\% \text{ year}^{-1}$). In contrast, whole column-integrated DIP had no important change and a ‘likely’ decrease ($-2.1\% \text{ year}^{-1}$) in the upper column. DOP was less abundant than DIP (Table S1A) and had a

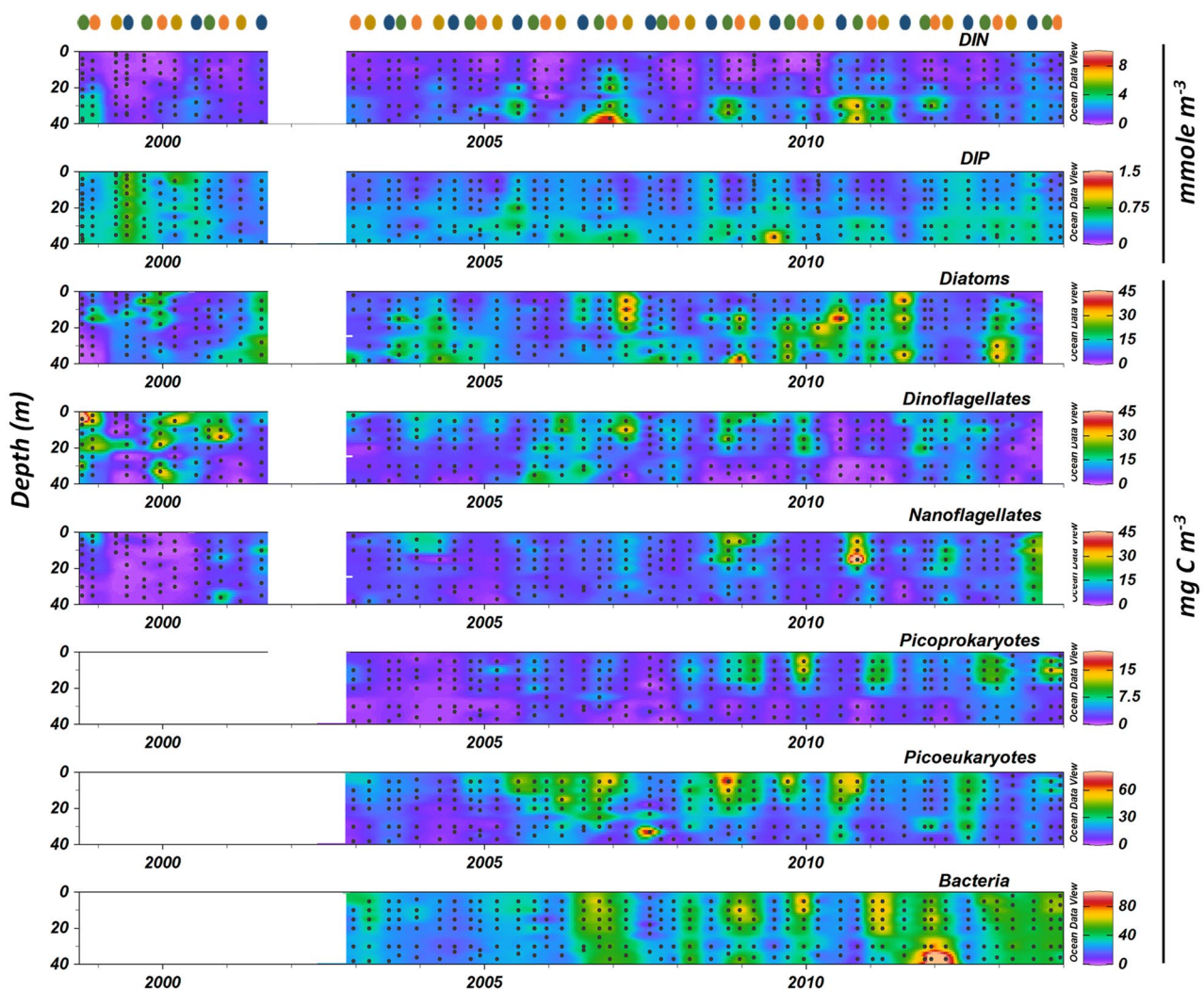


Fig. 2 Concentrations of dissolved inorganic N (DIN) and P (DIP) (mmol m^{-3}) and microplankton groups (mg C m^{-3}) from CTD-rosette water samples at the Firth monitoring site (Fig. 1), plotted by depth and time from September 1998 to December 2013. Coloured dots

denote seasons: green (spring), orange (summer), yellow (autumn) and blue (winter). Ticks on the x-axis correspond to 1 January of each year. Depths sampled are shown by black dots. Sampling was not carried out between July 2001 and December 2002

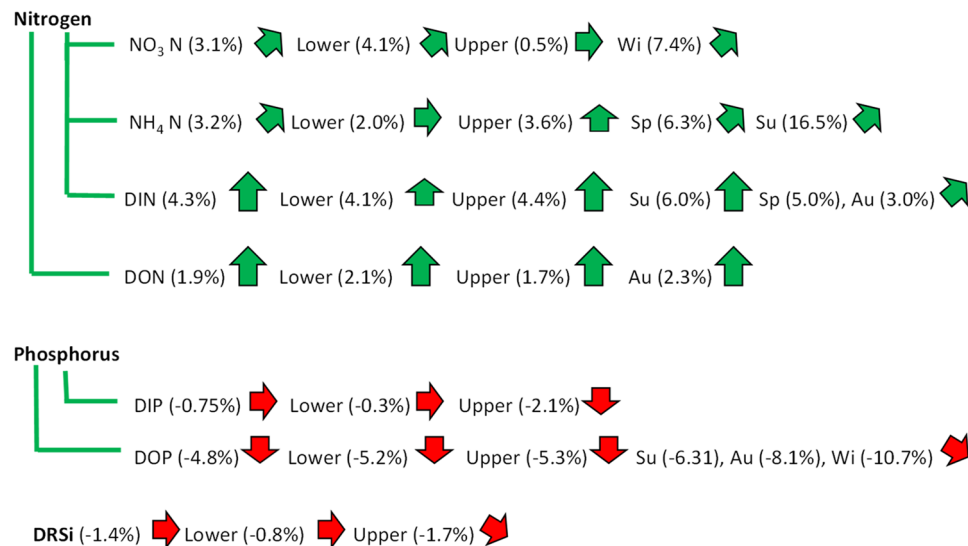


Fig. 3 Likelihoods and strengths of temporal trends for nutrient concentrations (mmol m^{-2}) determined using seasonal Kendall trend tests. The first arrow in each row shows trend direction and likelihood for concentrations integrated over the 40 m water column using the arrow symbols described in Table 1. Subsequent arrows in each row show trend results for concentrations integrated over upper (<20 m)

and lower (≥ 20 m) water column depth strata and seasons, for which trends were ‘possible’ or stronger in likelihood for 40 m integrated concentrations. Annotated percentages are percent annual changes of concentrations, and seasons are annotated as spring (Sp), summer (Su), autumn (Au) and winter (Wi)

column-integrated ‘possible’ decrease of $-4.8\% \text{ year}^{-1}$. DRSi had a weak ‘possible’ decrease in the upper water column ($-1.7\% \text{ year}^{-1}$) but otherwise did not change. Overall, during their 15.5-year time series, whole water column-integrated DIN and DON had increases of 99% and 34%, respectively. DRP and DRSi changed little and DOP decreased by 54%.

Autotrophic Trends

The biomasses of phytoplankton $> 2 \mu\text{m}$ and picophytoplankton ($< 2 \mu\text{m}$) groups over their respective time series at the monitoring site were generally the highest in the upper (<20 m) water column (Fig. 2) that corresponded with persistently depleted DIN concentrations at those depths. On occasion, biomass was distributed more evenly throughout the water column or concentrated in the lower column (≥ 20 m), particularly for diatoms. There was a pattern for dinoflagellates to be more abundant than diatoms early in the time series period, but this pattern reversed later in the period (Fig. 2).

Over their 15-year time series, column-integrated total phytoplankton $> 2 \mu\text{m}$ biomass had a ‘very likely’ increase ($2.5\% \text{ year}^{-1}$; Fig. 4A; Table S2A). Within the phytoplankton $> 2 \mu\text{m}$ group, diatom biomass had a ‘possible’ increasing trend ($3.9\% \text{ year}^{-1}$). Among diatoms, centric diatoms had a strong ‘likely’ increase ($4.2\% \text{ year}^{-1}$), pennate diatoms had a ‘possible’ increase ($2.1\% \text{ year}^{-1}$), and toxic diatoms had a very strong ‘virtually certain’ increase ($13\% \text{ year}^{-1}$).

Overall, predominately increasing trends occurred within the diatom populations (Fig. 4A). Total dinoflagellates, on the other hand, had a ‘possible’ decreasing trend ($-3.9\% \text{ year}^{-1}$; Fig. 4A; Table S2A). Within that group, armoured dinoflagellates had no likely change, while naked and toxic dinoflagellate biomasses had a ‘virtually certain’ decrease ($-4.5\% \text{ year}^{-1}$) and ‘possible’ decrease ($-4.6\% \text{ year}^{-1}$), respectively. Nanoflagellates had a ‘virtually certain’ increase ($5.7\% \text{ year}^{-1}$). Within the picophytoplankton time series, picoprokaryotes (*Synechococcus* dominated) had a ‘virtually certain’ increasing biomass ($11.5\% \text{ year}^{-1}$), while picoeukaryotes had no likely change (Fig. 4A; Table S2A).

Separate trend analyses of biomasses integrated over upper (<20 m) and lower (≥ 20 m) water column strata (Fig. 4A; Table S2B) showed that total phytoplankton $> 2 \mu\text{m}$ biomass increases were stronger in the lower column than the upper column (‘very likely’ vs ‘possible’ increasing trends, respectively). Total diatom biomass had a weak ‘possible’ increasing trend in the lower water column ($3.8\% \text{ year}^{-1}$) and no likely trend in the upper water column. Large centric diatoms, however, had a stronger ‘increasing trend likely’ ($5.1\% \text{ year}^{-1}$) in the lower column. Pennate diatoms had an ‘increasing trend possible’ in the lower column and upper column, increasing $2.5\% \text{ year}^{-1}$ and $2.9\% \text{ year}^{-1}$, respectively. Toxic diatoms in the lower column had a ‘virtually certain’ increasing trend ($14.5\% \text{ year}^{-1}$) and a ‘very likely’ increasing trend ($11.2\% \text{ year}^{-1}$) in the upper column. Total dinoflagellates had no likely trend in the lower column and a ‘possible’ decreasing trend in the upper column,

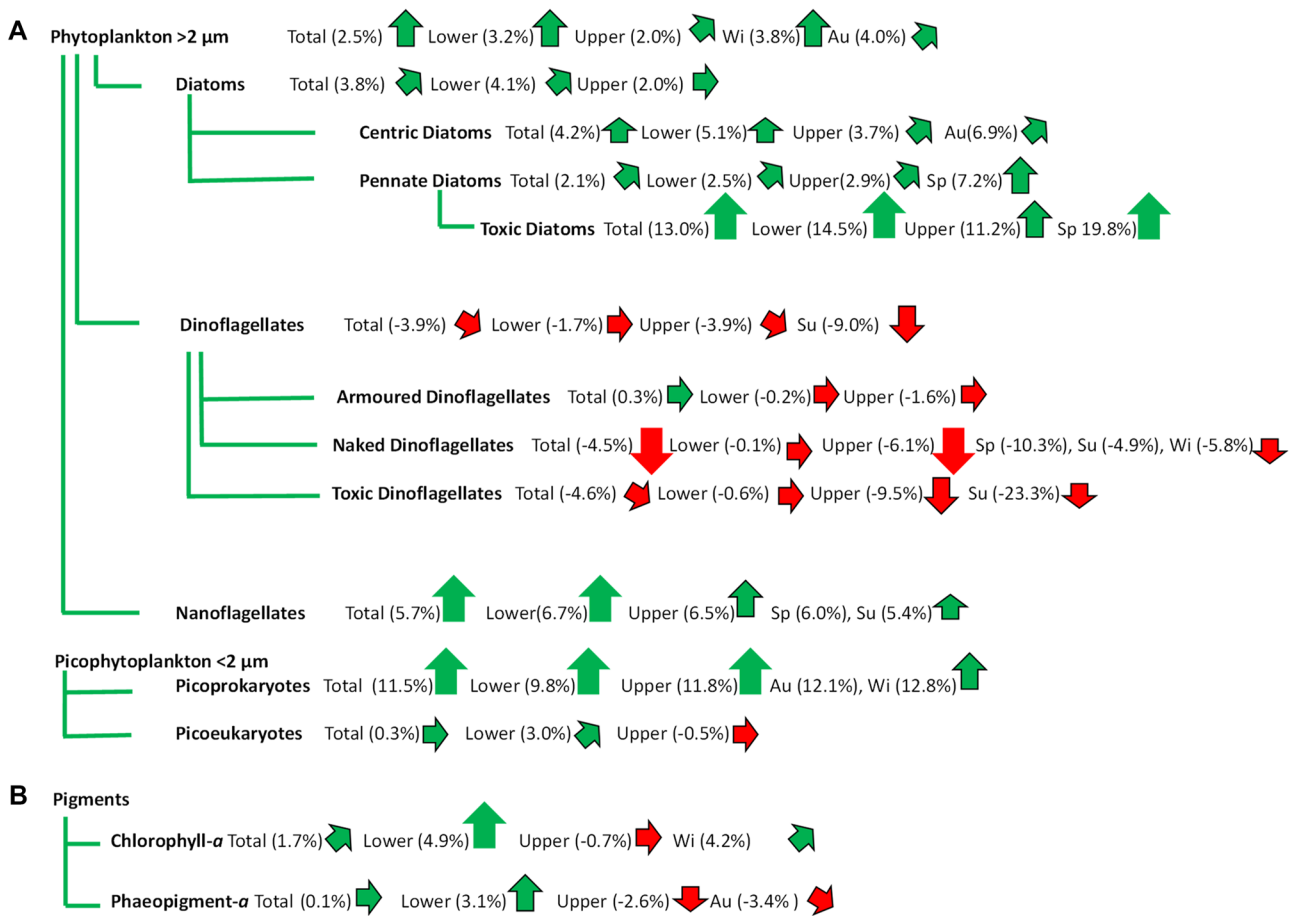


Fig. 4 Likelihoods and strengths of temporal trends for concentrations of **A** phytoplankton (mg C m^{-2}) and **B** chlorophyll *a* and phaeopigment-*a* (mg pigment m^{-2}), determined using seasonal Kendall trend tests. The first arrow in each row shows direction and likelihood of change in total biomass of the groups integrated over the 40 m water column, using the arrow symbols described in Table 1. Subse-

quent entries in each row show trend results for biomass integrated over lower (≥ 20 m) and upper (< 20 m) water column depth strata and seasons for which trends were ‘possible’ or stronger in likelihood, for 40 m integrated biomass. Annotated percentages are percent annual changes of biomass, and seasons are annotated as spring (Sp), summer (Su), autumn (Au) and winter (Wi)

while armoured dinoflagellates had no likely trends. Naked and toxic dinoflagellates had no trends in the lower column but ‘virtually certain’ and ‘very likely’ decreases ($-6.1\% \text{ year}^{-1}$, $-9.5\% \text{ year}^{-1}$, respectively) in the upper column. Nanoflagellates had a ‘virtually certain’ increasing trend in the lower column ($6.7\% \text{ year}^{-1}$) and ‘very likely’ increase in the upper column ($6.5\% \text{ year}^{-1}$). Picoprokaryotes had ‘virtually certain’ increasing trends in both lower ($9.8\% \text{ year}^{-1}$) and upper water columns ($11.8\% \text{ year}^{-1}$), while picoeukaryotes had a ‘possible’ increase (3.0%) in the lower column.

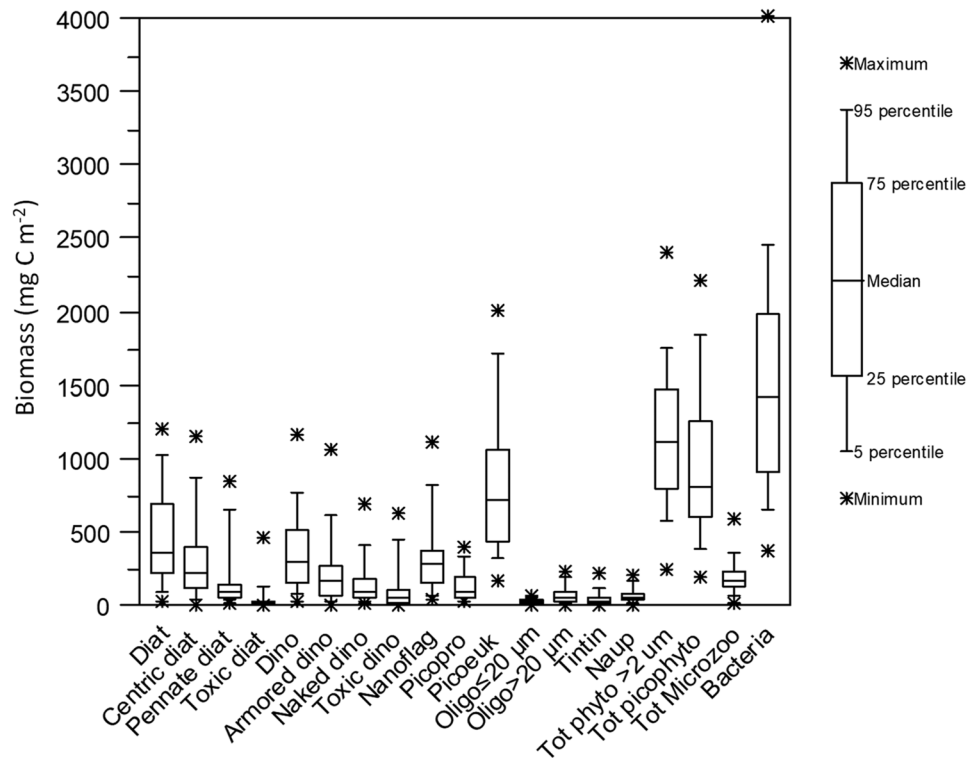
Seasonal trend analyses (Fig. 4A; Table S3C) showed that total phytoplankton $> 2 \mu\text{m}$ biomass increases were driven most by increases in autumn ($4.0\% \text{ year}^{-1}$) and winter ($3.8\% \text{ year}^{-1}$). Total diatoms trends were not affiliated with any season, but centric diatoms increases were linked with autumn (‘possible’, $6.9\% \text{ year}^{-1}$), while pennate and toxic diatoms increased in spring (‘very likely’, $7.2\% \text{ year}^{-1}$ and ‘virtually certain’ $19.8\% \text{ year}^{-1}$, respectively).

Decreases of total dinoflagellates were ‘very likely’ ($-9.0\% \text{ year}^{-1}$) in summer, with naked dinoflagellates having ‘very likely decreasing’ trends (-10.3 , -4.9 and $-5.8\% \text{ year}^{-1}$) in spring, summer and winter, respectively. Toxic dinoflagellates decreased most in summer (‘likely’, $-23.3\% \text{ year}^{-1}$). Nanoflagellates had their strongest increases in spring and summer (‘likely’, 6.0 and $5.4\% \text{ year}^{-1}$, respectively). Picoprokaryotes increased most in autumn and winter (‘very likely’, 12.1 and $12.8\% \text{ year}^{-1}$, respectively).

Phytoplankton $> 2 \mu\text{m}$ biomass integrated over the whole 40 m water column increased by 46% between 1998 and 2013. Within that group, diatoms increased by 57% (including centrics, which increased by 93%), and nanoflagellates, which increased by 151%, while dinoflagellates decreased by 46%. Within the picophytoplankton, picoprokaryotes increased by 369%, while picoeukaryotes changed little.

Median values of the taxonomic group biomasses at their time series midpoints (Fig. 5) showed that diatoms,

Fig. 5 Median biomasses (mg C m^{-2}) of phytoplankton $> 2 \mu\text{m}$, picophytoplankton and heterotrophs integrated over the whole water column, at mid-points of their respective time series



dinoflagellates and nanoflagellates contributed roughly equal proportions to total phytoplankton $> 2 \mu\text{m}$. The diatoms were composed mostly of centric types, dominated by several large genera, including *Coscinodiscus*, *Trieres* (formerly *Odontella*), *Rhizosolenia*, *Proboscia*, *Thalassiosira* and *Chaetoceros*. Pennate diatoms were less abundant than the centrics and were mainly *Pseudo-nitzschia*, *Nitzschia* and *Navicula*. The toxic diatoms were *Pseudo-nitzschia* and were rare overall but occasionally abundant in spring. Dinoflagellates were mostly armoured, followed by naked types, the latter contributing most to the overall declining dinoflagellate biomass trends (Fig. 4A). The declining toxic dinoflagellate group included the genera *Karenia*, *Alexandrium*, *Dinophysis*, *Gonyaulax*, *Lingulodinium* and the less common *Ostreopsis* and cf. *Gambierdiscus*. Nanoflagellates contributed strongly to the increasing phytoplankton $> 2 \mu\text{m}$ biomass (Fig. 4A) and were dominated by monads, Cryptophyceae, Chrysophyceae and Prymnesiophyceae with occasional euglenoids, silicoflagellates, *Octactis/Dictyocha* and toxic raphidophytes *Heterosigma*, *Fibrocapsa*, *Chattonella* and *Prymnesium*. There were only three instances when any of the toxic components of the nanoflagellates contributed more than 0.1% of biomass (not shown in Fig. 5). The picoprokaryotes, while increasing strongly over the time series, contributed relatively little to overall phytoplankton biomass ($\sim 6\%$ on average) (Fig. 5). In contrast, the picoeukaryotes, while having few important biomass

trends (Fig. 4A), contributed substantial biomass, comparable to the summed biomasses of diatoms, dinoflagellates and nanoflagellates.

Chl-*a* pigment (Fig. 4B), integrated over the whole 40 m water column, had a ‘possible’ increase ($1.7\% \text{ year}^{-1}$), while its degradation product, phaeo-*a*, had no important trend (Fig. 4B; Table S3A). However, chl-*a* and phaeo-*a* had ‘virtually certain’ and ‘very likely’ increases in the lower water column, (4.9 and $3.1\% \text{ year}^{-1}$, respectively). In the upper column, chl-*a* had no trend, and phaeo-*a* had a ‘likely’ decrease. Seasonal patterns for pigments integrated over the whole water column were weak with only ‘possible’ increases in winter for chl-*a* and in autumn for phaeo-*a*.

The increases of pigments in the lower water column reflected the increases seen in total phytoplankton $> 2 \mu\text{m}$, particularly centric diatoms and nanoflagellates (Fig. 4A). While chl-*a* integrated over the whole water column increased by only 31% and phaeo-*a* had little change, chl-*a* and phaeo-*a* integrated over the lower water column ($\geq 20 \text{ m}$) increased by 123 and 63%, respectively.

Heterotrophic Trends

Water column-integrated bacterial biomass had a ‘virtually certain’ increasing trend ($5.5\% \text{ year}^{-1}$) and ‘virtually certain’ and ‘very likely’ increasing trends when divided into the lower and upper water columns ($5.5\% \text{ year}^{-1}$, $6.8\% \text{ year}^{-1}$, respectively) (Fig. 6; Table S4A, B). Bacterial increases

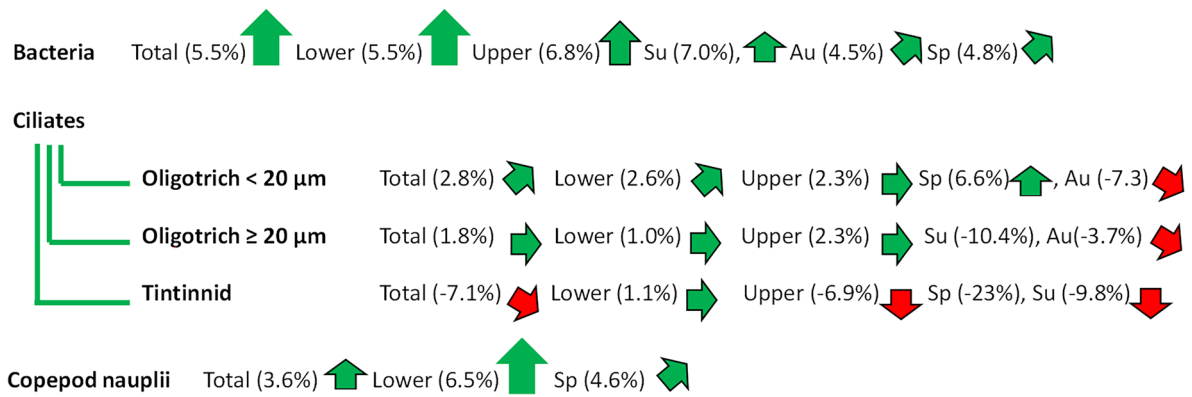


Fig. 6 Likelihoods and strengths of temporal trends for heterotrophs (mg C m^{-2}), determined using seasonal Kendall trend tests. The first arrow in each row shows direction and likelihood for biomass of the groups integrated over the 40 m water column, using the arrow symbols described in Table 1. Subsequent arrows in each row show trend results integrated over lower (≥ 20 m) and upper (< 20 m) water

column depth strata and seasons for which trends were ‘possible’ or stronger in likelihood, for 40 m integrated biomasses. Annotated percentages are percent annual changes of concentrations, and seasons are annotated as spring (Sp), summer (Su), autumn (Au) and winter (Wi)

were strongly linked to summer with a ‘likely’ $7.0\% \text{ year}^{-1}$ increase, but there were also ‘possible’ increases in spring and autumn (Fig. 6; Table S4C). The small oligotrich ($< 20 \mu\text{m}$) biomass integrated over the whole column had a ‘possible’ increasing trend ($2.8\% \text{ year}^{-1}$), mainly in the lower water column (‘possible’, $2.6\% \text{ year}^{-1}$). They had a ‘likely’ increase in spring ($6.6\% \text{ year}^{-1}$), but a ‘possible’ decrease in summer ($-7.3\% \text{ year}^{-1}$). Larger $> 20 \mu\text{m}$ oligotrichs had no important trends, while tintinnids had ‘possible’ decreasing biomass which was focused in the upper water column (‘likely’, -6.9%) in spring (‘likely’, -23%). Copepod nauplii had a ‘likely’ increase ($3.6\% \text{ year}^{-1}$), which was focused in the lower water column ($6.5\% \text{ year}^{-1}$ ‘virtually certain’) (Table S4). Over their respective time series, bacteria column-integrated biomass increased by 89% during 2002 to 2013, while over the 1998–2013 period smaller ($< 20 \mu\text{m}$) oligotrich biomass increased by 53%, larger tintinnids decreased by 69% and nauplii increased by 73%. The biomasses of heterotrophic groups (bacteria, ciliates, nauplii: Fig. 5) showed that bacteria biomass dominated the heterotrophic community and rivalled the total autotrophic (phytoplankton $> 2 \mu\text{m}$ + picophytoplankton) biomass.

Drivers of Biomass

Multivariate GAM analysis identified DIN concentration and stratification as having the strongest relationships with phytoplankton and bacterial biomasses, with DIN identified as the dominant driver and stratification secondary as shown by the higher F ratios and p values for DIN (Table 2). Concurrency or collinearity of variables showed that model parameters were between 0.72 and 0.76 (values close to one indicate redundancy), with DIN showing

the least covariance with other parameters (Table 2). Bacteria, diatoms, picoeukaryotes and nanoflagellates all had increasing linear or saturating relationships with increasing DIN (Fig. 7), while dinoflagellates and picoprokaryotes had decreasing relationships. Factors with poor explanatory power that were dropped from the analysis were DON, small and large oligotrichs and nauplii. Lagging the GAM model by one season (i.e., *ca* 3 months) with respect to biomass (not shown) yielded poorer fits than the non-lagged model, with adjusted r^2 dropping from 0.63 to < 0.10 . Given the likely quick responses of biomass to changes in nutrient and physical conditions (days rather than months), this is not unexpected.

Table 2 General Additive Model (GAM) output for assessing the influence of water column-mean values of physical properties, temperature ($^{\circ}\text{C}$), salinity (psu), density stratification (Brunt-Väisälä frequency: cycles h^{-1}) and water column-integrated nutrient concentrations (mmol m^{-2}) on microbial plankton biomasses (mg C m^{-2}) over seasonal surveys 1998–2013. Parameters significantly related to biomass ($p < 0.05$) are highlighted in bold. The table includes diagnostics of the relationship between each parameter and biomass (*Edf* estimated degrees of freedom, *Ref.df* reference degrees of freedom, *F* and *p* value) and the concurrency estimate for each parameter (Wood 2006). The overall model fit had an adjusted r^2 of 0.63 and 62.4% deviance explained. Categorical comparisons between categorical factors ‘microbial plankton group’ and ‘season’ are given in Table S5

Parameters	Edf	Ref.df	<i>F</i>	<i>p</i>	Concurrency
DIN	1.6	9	0.77	0.008	0.72
Stratification	0.8	9	0.37	0.04	0.75
DIP	0.6	9	0.2	0.10	0.76
Temperature	0.0001	9	0.0	0.50	0.76
Salinity	0.00009	9	0.0	0.88	0.75

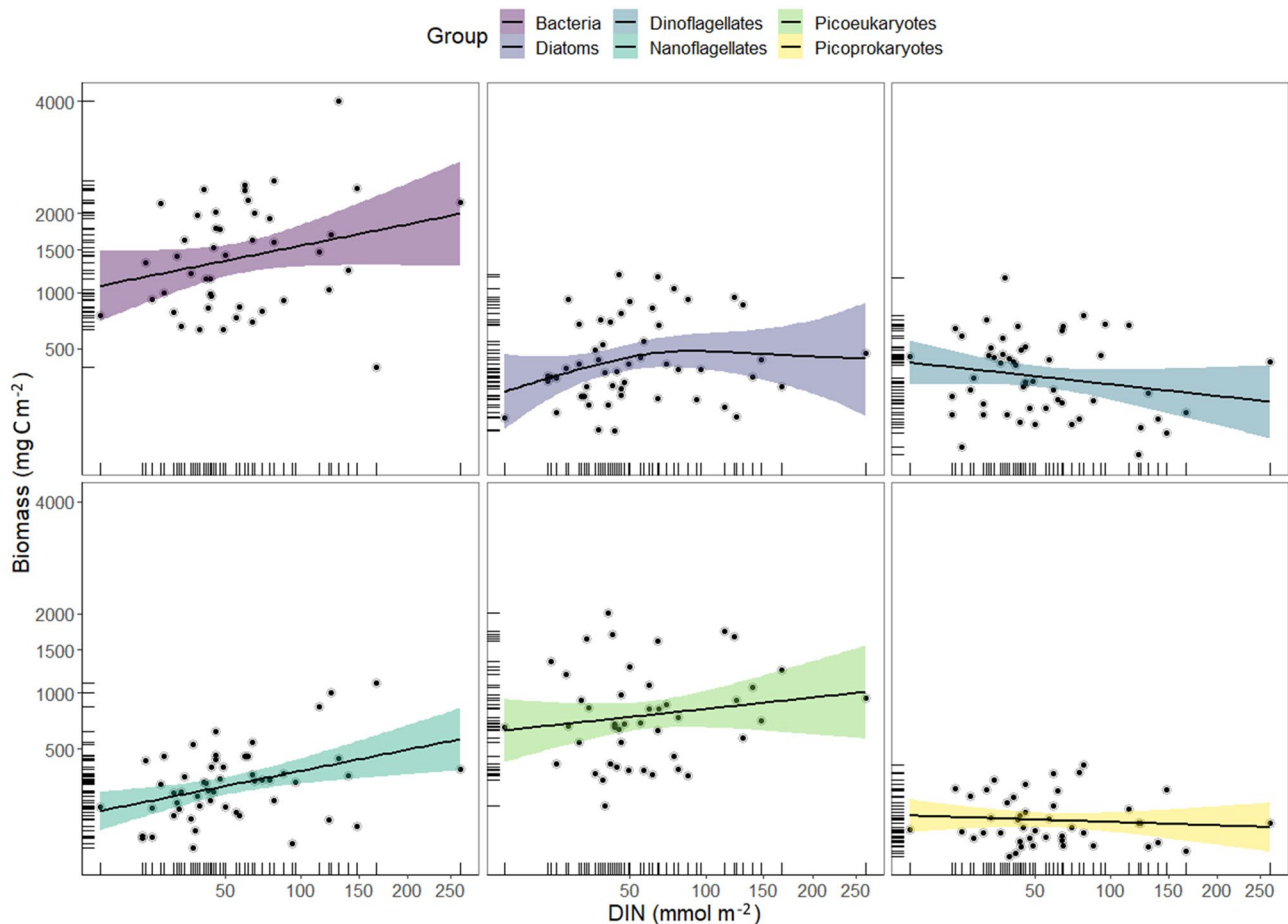


Fig. 7 Relationship between DIN concentration (mmol m^{-2}) and water column-integrated biomass (mg C m^{-2}) of phytoplankton taxonomic groups and bacteria. Regressions are fitted using General Additive Models (± 0.95 CI). *x*- and *y*-axis are square root-transformed

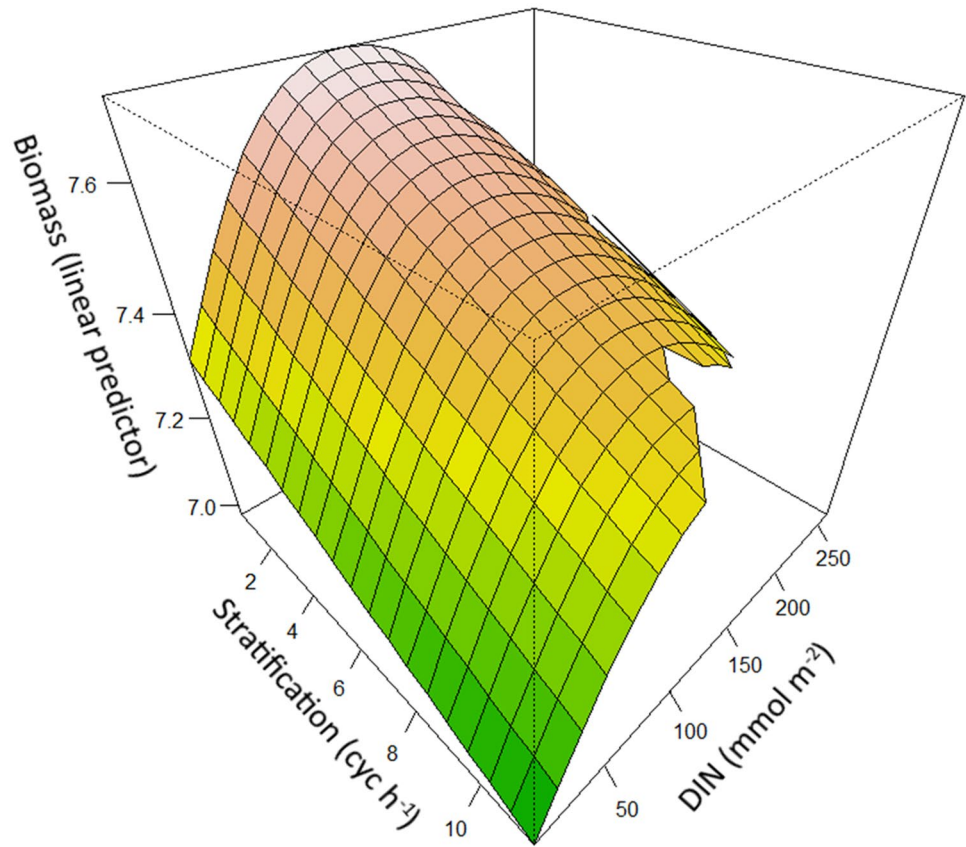
The interactive effects of DIN and stratification on biomass (Fig. 8) showed that under strong (high values) water column stratification and low DIN concentrations, biomass was highly suppressed. However, increases in DIN were associated with strong increases in biomass across the full range of stratification values. Overall, the relationship predicted a saturation of biomass increase at DIN concentrations between 100 and 150 mmol m^{-2} , although inferred declines in biomass beyond these concentrations were described by increasingly sparse data points (Fig. 8). To further isolate the relative effects of DIN and stratification on biomass, inter-annual and intra-annual (seasonal) variations in these parameters were considered. While DIN was shown to have a ‘very likely’ increasing inter-annual trend (Fig. 3, Table S1), water column temperature, salinity and stratification all had ‘unlikely’ trends (Table 3). However, stratification varied significantly intra-annually (between seasons), while DIN had no significant seasonal variation (Table 4). These results indicated that the DIN effect on biomass detected by the GAM arose primarily via its strong

increasing trend over the 15-year time series, whereas the relatively weak effect of stratification on biomass arose at shorter time scales, potentially via stochastic, year-to-year variability and intra-annual seasonal variation.

Comparison of categorical factors ‘microplankton group’ and ‘season’ used in the GAM to predict effects of nutrient and physical variables on biomass showed that effects due to factor ‘microplankton group’ were stronger ($p < 0.001$) than effects due to factor ‘season’, which were largely non-significant (Table S5). The relatively strong effects of ‘microplankton group’ likely arose from the contrasting responses of diatom, nanoflagellate, picoeukaryote and bacteria groups (increasing biomass) and the dinoflagellate group (decreasing biomass) to increasing DIN (Fig. 7). The relatively weak response to factor ‘season’ was likely due to lack of biomass variations across seasons which were largely non-significant, apart from that of picoeukaryotes (Table 4).

The seasonal surveys made in 2012–2013 and in 2010 which traversed the Firth (Fig. 9) showed that chl-*a* and phaeo-*a* decreased in the upper column (< 20 m) and

Fig. 8 Interactive response of phytoplankton/bacteria biomass (as predicted by General Additive Models: green = low, orange = high biomass) to DIN concentration (mmol m^{-2}) and water column stratification (Brunt-Väisälä frequency: cycles h^{-1} ; higher values mean more strongly stratified)). Fitted mesh is constrained to interpolate 25% beyond actual data



increased in the lower column between spring and summer. These patterns were reflected by increased transmittance in the upper water column and decreased transmittance in the lower column. Nitrate was depleted to low levels ($\leq 0.5 \text{ mmol m}^{-3}$) in the upper water column from spring through autumn, accompanied by strengthening stratification spring to summer. The deeply distributed biomass in summer was accompanied by increased $\text{NH}_4^+\text{-N}$ and decreased O_2 , indicating that it was senescing and mineralising. Inter-annual variation in the seasonal occurrence of these processes was seen by comparing the surveys in summer 2013 and autumn 2010 (Fig. 9) that showed similar chl-*a*, phaeo-*a*, transmittance, stratification and O_2 patterns but with a seasonal shift.

Table 3 Seasonal Kendall time trend tests for water column median temperature ($^{\circ}\text{C}$), salinity (psu) and density stratification (Brunt-Väisälä frequency: cycles h^{-1}). Shown are numbers of seasons sampled, the median value over 1998–2013 time series, the significance

Variable	<i>N</i>	Median value	Kendall P	% annual change	Sen's slope	90% c.l. for slope	Slope direction probability	Trend direction and confidence
Temperature	58	15.957	0.939	-0.013	-0.002	-0.049 to 0.042	0.546	Trend extremely unlikely
Salinity	58	34.893	0.98	0.001	0.000	-0.009 to 0.011	0.520	Trend exceptionally unlikely
Stratification	58	4.703	0.778	0.538	0.025	-0.094 to 0.122	0.620	Trend unlikely

Discussion

Inter-annual and Seasonal Dynamics of Microplankton Biomass

The 15-year trend analyses showed increasing DIN coincided with increases in several auto- and heterotrophic group biomasses, while the GAM analysis identified DIN increase as the dominant correlate of biomass changes, with stratification secondarily important. While having a strong increasing trend over the time series, DIN trends did not vary significantly between seasons (Table 4), indicating that it affected biomass primarily via its long-term trend over the time series, across all degrees of

level of trend slope (Kendall P), the % annual change, the Sen slope, 90% confidence limits of the slope, the probability that the slope was truly above or below zero and confidence of trend direction

Table 4 Seasonal water column median values of column-integrated physical properties (temperature ($^{\circ}\text{C}$), salinity (psu), density stratification (Brunt-Väisälä frequency: cycles h^{-1}), nutrients (mmol m^{-2}) and microbial biomasses (mg C m^{-2}) examined in the GAM analysis. For each variable, seasonal values with different letters were significantly different ($p < 0.05$; Kruskal–Wallis multiple comparisons, with Kruskal–Wallis p given). Variables with significant seasonality are highlighted in bold. Seasons were austral spring, September–November; summer, December–February; autumn, March–May; winter, June–August

	Spring	Summer	Autumn	Winter	K-W p
Temperature	14.7 a	17.4 b	20.7 b	14.1 a	0.00
Salinity	34.6 a	35.0 b,c	35.2 b	34.8 a, c	0.00
Stratification	5.8 a,b	7.2 a	3.6 b,c	2.4 c	0.00
DIN	39.5 a	61.4 a	38.4 a	57.8 a	0.22
DIP	15.2 a	13.9 b	14.8 a	19.6 a	0.01
Diatoms	261 a	445 a	381 a	328 a	0.32
Dinoflagellates	410 a	445 a	218 a	235 a	0.09
Nanoflagellates	278 a	296 a	232 a	262 a	0.82
Picoprokaryotes	154 a	109 a	114 a	63 a	0.22
Picoeukaryotes	928 a	515 b	642 a	881 a	0.03
Bacteria	1423 a	1760 a	1769 a	991 a	0.10

stratification (Fig. 8). This association with DIN was consistent with findings in coastal ecosystems showing that biomass is demonstrably related to nutrient loading rates

and concentrations (Boynton and Kemp 2008; Boynton et al. 1982; Monbet 1992), albeit with variability in the relationships across different types of coastal ecosystems (Cloern and Jassby 2008). The long residence times and relatively clear waters of large coastal embayments such as the Firth mean such systems are sensitive to nutrient enrichment (Zeldis et al. 2022). They are susceptible because, in addition to having potentially high nutrient loading from large catchments, they can support phytoplankton blooms which undergo complete cycles of growth, consumption and senescence, prior to seaward export (Ferreira et al. 2005).

Stratification had a significant but weaker effect than DIN, with increased stratification depressing microplankton biomass. This could be caused by decreased vertical flux of nutrients from the pycnocline into the mixed layer with increased stratification, an effect considered an important controlling factor in primary production in seasonally stratified coastal waters (Eppley et al. 1979; Mann and Lazier 1991). In the Firth, this may have operated at both inter-annual and intra-annual (seasonal) time scales, affecting biomass at both frequencies. Although stratification strength had no consistent trend over the 15-year time series (Table 3), it did vary from year to year at the Firth monitoring site, as shown by Zeldis and Swaney (2018) (their Fig. 9). This could have accounted for its effects on biomass

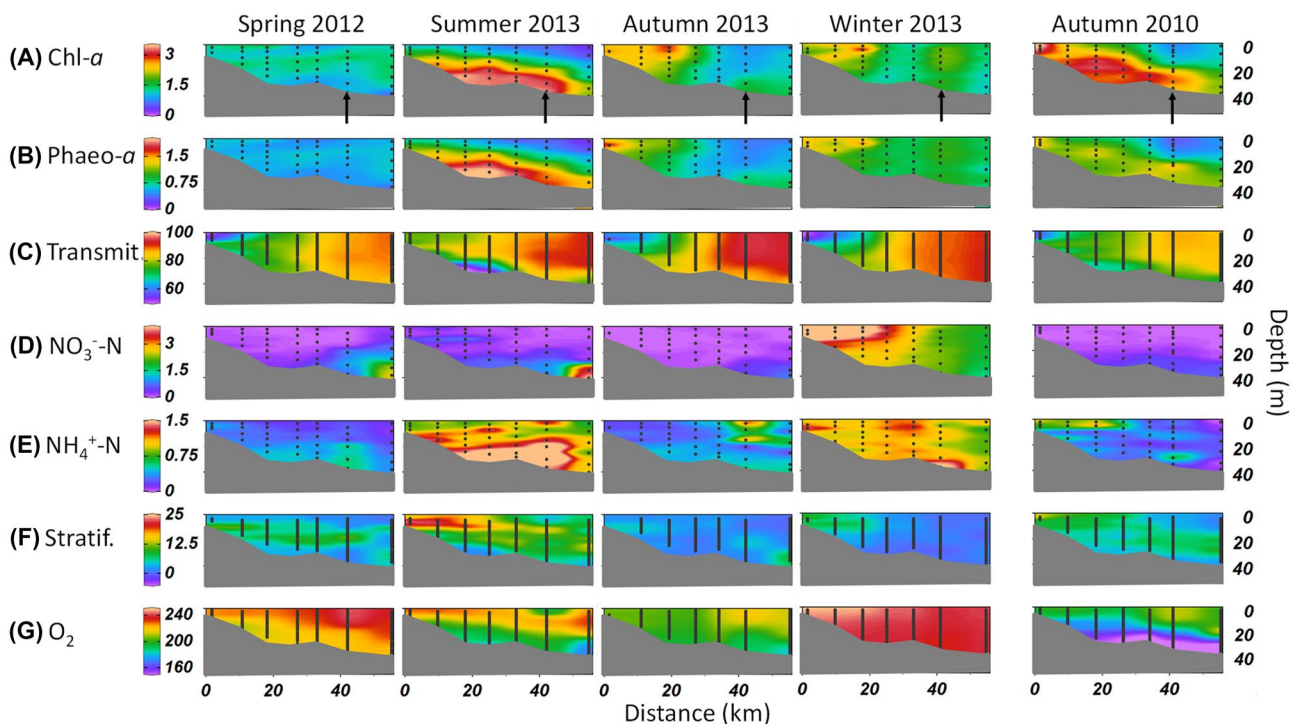


Fig. 9 Vertical sections of water column properties from the inner Firth into the Hauraki Gulf at stations in Fig. 1B, in spring, summer, autumn and winter 2012–2013 and autumn 2010. Properties are **A** chlorophyll *a* (chl-*a*) and **B** phaeopigment-*a* (phaeo-*a*) (mg m^{-3}), **C** water transparency (Transmit.) (%), **D** nitrate (NO_3^- -N) and **E** ammo-

nium (NH_4^+ -N) (mmol m^{-3}), **F** stratification (Brunt Väisälä frequency (cycles h^{-1} ; higher values mean more strongly stratified) and **G** oxygen (O_2 ; $\mu\text{mol kg}^{-1}$). Dots are depths of CTD bottle samples, and vertical lines are 1-m interval CTD-derived values. The arrows in the first row mark the location of the Firth monitoring site

in the GAM, albeit without a consistent trend over the whole time series. Stratification also varied strongly between seasons at the monitoring site (Table 4), as was also shown by seasonal surveys made along the length of the Firth (Fig. 9).

Linking Changes in the Microplankton Community to Nutrient Ratios

Changes in autotrophic and heterotrophic groups over their time series were accompanied by increasing trends in concentrations of DIN and DON at the Firth monitoring site. In contrast, DIP, DOP and DRSi had no trends or decreasing trends, resulting in changed ratios among the nutrient species. Nutrient ratios can affect phytoplankton composition because different taxonomic groups display differential preferences for specific nutrient ratios or nutrient forms, as proposed in the ‘nutrient ratio’ hypothesis (Smayda 1990, 1997; Tilman 1977). This suggested that the increase in the ratios of N to P and DRSi may have underpinned changes in biomass ratios among taxonomic groups. Increased diatom biomass and decreased dinoflagellate biomass during 1998–2013 (Figs. 2 and 4A) altered the ratio between these groups across the time series. The dominance of dinoflagellates at the start of the time series in 1998 resembled that sampled 2 years prior, in 1996–1997 (Chang et al. 2003), who reported a dominance of dinoflagellates over diatoms in the inner Hauraki Gulf. Dinoflagellates have a greater P requirement to support their maximum photosynthetic and respiration rates than other phytoplankton groups (Reynolds 2006). Increased N and stable or declining P resulted in an increasing N:P ratio that could have favoured other, less P-dependant groups, including diatoms. DOP concentrations declined, which also may have been a limiting factor because dinoflagellates can rely on DOP for nutrition (Lin et al. 2015). Silica was also sufficient for diatom growth, with Si:N ratio ~5:1, being far from limiting for diatoms (~1:1; Chang et al. (2003); Sarthou et al. 2005). The increasing biomass trends for larger diatoms were consistent with observations that N-stress relief during eutrophication can favour the growth of larger cells, based on cellular surface-to-volume considerations (Chisholm 1992; Philippart et al. 2000; Ragueneau et al. 1994; Stolte and Riegman 1995).

Nanoflagellates and bacteria also increased substantially over the time series, likely due to a combination of factors. Along with increased DIN supply, there was sufficient Si, which would benefit silico-flagellates and small Chrysophytes, which require adequate Si levels. Increasing DON would have also supported groups which can consume dissolved organic matter, like bacteria and some mixotrophic and heterotrophic flagellates, that can take up DON directly or via grazing (Antia et al. 1991; Berman and Bronk 2003; Flynn et al. 2019; Granéli et al. 1999; Sanderson et al. 2008; Seitzinger et al. 2002). The substantial increases of bacteria

and nanoflagellates over the time series were strong in summer and coincided with maximum increases in DIN, suggesting a strong trophic response was occurring through these groups.

Trophic Linkages Within the Microplankton Community

As well as microplankton community changes directly related to dissolved nutrient supply, other changes appeared related to trophic food-web linkages. Small heterotrophic and mixotrophic flagellates grazers are known to respond quickly to increases in bacteria and picoplankton (Capriulo et al. 2002; Duarte et al. 2000; Edwards 2019; Stoecker et al. 2017) and to act as primary consumers of those prey (Duarte et al. 2000; Flynn et al. 2019; Hall et al. 1993; Hansen et al. 1994; Safi and Hall 1999). Although we did not separately enumerate autotrophs, heterotrophs and mixotrophs in our nanoflagellates group, we assume that their strongly increasing biomass indicated that heterotrophy and mixotrophy were important in that group, as found in other coastal systems in New Zealand and elsewhere (Flynn et al. 2019; Riemann et al. 1995; Safi and Hall 1999; Unrein et al. 2007). Over the time series, DON increased most strongly in autumn, potentially from mineralisation of organic matter in summer and autumn (Fig. 3; Zeldis et al. (2022)). This mineralisation would be driven by bacteria, which increased strongly in summer, over the time series.

Naked dinoflagellates can also be important mixotrophic grazers (Lin et al. 2015) but their numbers declined. This may have been linked to their generally larger size. Mixotrophic dinoflagellates often have a 1:1 ratio in size, with respect to their prey (Hansen et al. 1994), indicating they would predominately consume mid-size prey (~20–40 µm). Prey of that size (i.e., Phytoplankton, ~20–40 µm) did not increase over the time series, unlike smaller nanoflagellates (dominated by 4–10 µm cells), bacteria, prokaryotic picoplankton (<2 µm) and oligotrichs <20 µm in size. Increased biomass of small (<20 µm) oligotrichs, in contrast, was potentially supported by the increased bacteria and picoprokaryotes (Christaki et al. 1999). Small oligotrichs graze primarily upon these very small prey, unlike larger (>20 µm) oligotrichs and tintinnids, which had little change or declined over the study period. Ciliates have an optimal prey-to-predator size ratio of about 18:1 (Hansen et al. 1994) indicating that while bacteria and picoplankton may have occupied a suitable prey size range for the smaller oligotrichs, they would not have been optimal for larger ciliates.

Interestingly, picoeukaryotes had a positive response to higher DIN concentration in the GAM analysis (Fig. 7) but little inter-annual trend over the time-series (Fig. 4A). Their response to DIN within the GAM was therefore likely due

to their relatively strong intra-annual (seasonal) response (Table 4), with wide variation across the seasons. The lack of inter-annual response by picoeukaryotes may be the result of tighter coupling between this population and nanoflagellate and oligotrich grazers, which often dominate grazing upon picoeukaryotes (Rassoulzadegan et al. 1988; Samuelsson and Andersson 2003). Picoeukaryotes are likely preferred by nanoflagellates and oligotrichs over picoprokaryotes or bacteria, because of their greater nutritional value (Monger and Landry 1991; Worden et al. 2004).

The weak increase of small ciliates and the lack of increase of larger ciliates may also be a function of top-down control by copepods. Strong predation pressure by copepods on ciliates is reported in subtropical waters east of New Zealand (Zeldis et al. 2002; Zeldis and Décima 2020), and Dolan (1991) reported strong predation pressure on ciliates by copepod nauplii in coastal waters (Chesapeake Bay, USA). These studies indicate that grazing on ciliates may have supported the increasing trend for copepod nauplii found in the present study.

Deleterious Algal Taxa and Phytoplankton Community Nutritional Quality

Nitrogen enrichment and changed nutrient ratios have been linked with increased occurrence of harmful algal blooms (Davidson et al. 2012; Glibert and Burford 2017). In this study, the toxic pennate diatom genus *Pseudo-nitzschia* spp. increased strongly (~4800%), mostly in spring, consistent with Rhodes et al. (2013) who found *Pseudo-nitzschia* spp. bloomed most commonly in spring and summer in NZ North Island coastal waters. In contrast, toxic dinoflagellate biomass declined, mainly in summer. Consideration of dissolved nutrient ratios may again help to explain these changes. As discussed, dinoflagellate growth is optimised at low N:P ratios (Hodgkiss and Ho 1997), but trends in the Firth indicated increasing N:P ratios. In the Gulf of Mexico, *Pseudo-nitzschia* spp. cell counts increased in parallel with increased NO_3^- -N loading over several decades (Parsons et al. 2002; Turner and Rabalais 1991). Our survey has shown that *Pseudo-nitzschia* spp. biomass increased in the Firth, and, if this trend continues, it may become more problematic given the most toxic strain (*P. australis*) is reported in this region (Rhodes et al. 2013).

The trends of declining dinoflagellates and increasing diatoms which we observed over this time series could indicate a shift in nutritional quality of the phytoplankton for grazers at higher trophic levels. Dinoflagellates and nanoflagellates have been shown to be considerably more nutritious than diatoms (in terms of C and N constituents) on a chl-*a* or volume-specific basis (Chan 1980; Hitchcock 1982; Rey et al. 2001), suggesting that the higher densities of dinoflagellates at the start of the time series would have been more

favourable for secondary production than later. It was previously shown that the planktonic system of the Hauraki Gulf had greater production of mesozooplankton and larval fish in years with higher dinoflagellate than diatom composition (Zeldis et al. 2005). The present results may indicate that N enrichment has set conditions for a less nutritious environment for mesozooplankton in the Firth. This may have been offset, however, by the increases of nanoflagellates and small ciliates, which can be passed quickly through nauplii and larger microzooplankton (Dolan 1991; Samuelsson and Andersson 2003).

Role of Microplankton in Nutrient Enrichment and Eutrophication

The results showed that increased microplankton biomasses and changed taxonomic group composition accompanied the changed nutrient environment (strong increases in N, no change or decreases in P) over the 1998–2013 period. In the case of P, concentrations declined slightly in the Firth river inputs during the period (by ~0.6–1.5% year⁻¹ Vant (2013)), likely driven by point source improvements in the catchment, consistent with the flat or decreasing trends in DIP and DOP in the Firth. For N, Zeldis and Swaney (2018) described the balance of offshore- and catchment-derived N supply to the system. They showed that neither offshore physical oceanographic conditions (upwelling) nor enhanced estuarine exchange changed within the Hauraki Gulf/Firth system, indicating these factors were unlikely to be drivers of changed N. Changes in water quality in the Firth river inputs also were not strong drivers of changed N loading, with only small increases in river TN concentrations (maximum 1.7% year⁻¹: Vant (2013); Zeldis and Swaney (2018)), much less than the strongly increasing trends of DIN and DON over the period. Thus, there was little evidence of either offshore-or catchment-side change during the monitoring period that would explain the N and microplankton biomass increases in the Firth.

Another potential explanation for the observed N enrichment is changed internal nutrient cycling in the Firth sediments, related to denitrification. The nutrient mass-balance analysis of Zeldis and Swaney (2018) found that the denitrification rate in the Firth decreased by ~58%, between surveys made in 2000–2001 and 2012–2013. Studies made elsewhere have shown that the denitrification rate can be inhibited by organic enrichment in sediments (Cook et al. 2004; Eyre and Ferguson 2009; Hale et al. 2016; Harris et al. 1996; Kemp et al. 1990; Tait et al. 2020), raising the possibility that organic enrichment of sediments could have decreased denitrification and increased availability of DIN to primary producers, thus driving a positive feedback on eutrophication. This was supported by sediment biogeochemistry studies made at the Firth monitoring site in 2003

and 2012 (Zeldis and Swaney 2018), showing that sediment O_2 demand increased over that period by ~1.5 to 1.7-fold, indicating organic enrichment.

Water column N enrichment can enhance downward transport of phytoplankton, leading to enrichment of sediments (Kemp et al. 2005; NRC 2000). This is due not only to higher algal production generally, but also shifts toward larger algal species with higher sedimentation characteristics (Philippart et al. 2000). In the Firth, larger taxa (phytoplankton $> 2 \mu\text{m}$) were important contributors to total phytoplankton biomass (Fig. 5) and had increasing trends (Fig. 4A). This was particularly the case for large centric diatoms, which had their largest increases in autumn, toward the end of the production season. Nanoflagellate biomass also increased in spring and summer throughout the water column, adding to organic enrichment. These increases were reflected by increased chl-*a* and phaeo-*a* in the lower column over the time series. The increases of large-celled phytoplankton and nanoflagellates were accompanied by elevated DON and bacteria, again in summer/autumn, indicating linkage between autotrophs and heterotrophic activity toward the end of the production season. The increasing biomasses during the time series of larger phytoplankton more prone to sedimentation suggested that deposition of biomass to sediments may have increased over the period, supported by the observations of increased sediment O_2 demand (Zeldis and Swaney 2018). Thus, enhanced organic matter deposition and enrichment of the sedimentary environment may have underlain decreased denitrification and increased availability of DIN to primary producers.

In the Firth, primary biomass and its mineralisation increased in the lower water column late in the production season, as shown by the elevated concentrations of chl-*a*, its degradation product (phaeo-*a*), and decreased O_2 in the lower water column between spring and summer (Fig. 9). These findings were consistent with the summer/autumn low O_2 regularly recorded in the lower half of the water column at the monitoring site over 1998–2013 (Zeldis and Swaney 2018). The results of Fig. 9 do not distinguish whether the deep biomass was the result of increased export from the upper water column or simply decreased production in surface waters and increased production at depth. However, while phytoplankton biomass has little seasonal variation in the Firth (Table 4), integrated net primary production (NPP) increases between spring and summer in the inner Hauraki Gulf and Firth (Bury et al. 2012; Gall and Zeldis 2011). This suggests that biomass turnover and export from the euphotic zone is likely to increase between spring and summer. This conforms with observations in Yangtze River estuary (China: Zhou et al. 2020), where low O_2 in bottom waters was driven by respiration of diatom-rich phytoplankton settling through the pycnocline in summer/autumn. In the Firth, the seasonal dynamics of biomass turnover is an

important topic for future research, because of its association with expression of ecological stressors (acidification and hypoxia) as described by Zeldis et al. (2022). The increasing trends over 1998–2013 for larger phytoplankton taxa prone to sedimentation indicated potential for increased deposition of organic matter that could explain the biogeochemical changes (reduced denitrification and increased sediment O_2 demand) observed over the period (Zeldis and Swaney 2018).

Unlike the trends in DIN and microplankton, the 1998–2013 time series of water column O_2 at the monitoring site showed no important trend, with ‘increasing trend about as likely as not’ (not shown). The lack of consistent trend in water column O_2 could have arisen from the complex interacting factors that affect O_2 concentrations in the coastal sea, including stratification, air-sea exchange and degree of organic matter production (Hagy et al. 2004; Scully 2016), as was evident in the variable chl-*a*, stratification and O_2 we observed between autumn 2010 and autumn 2013 (Fig. 9). Irrespective, O_2 levels during 1998–2013 at the Firth site often reached 60% O_2 saturation and occasionally 40% (Zeldis and Swaney 2018). Thus, while the DIN and microplankton increases observed over 1998–2013 did not result in a worsening of hypoxia, they did indicate a furthering of the enrichment the Firth has received over multiple decades (Introduction) that drives frequent expression of low O_2 .

Summary and Conclusion

Our study has used a combination of time series and GAM analyses showing the key role of N enrichment in driving microplankton biomass increase over a decadal-scale time series, with weaker effects of stratification operating at shorter time scales. Important increases occurred for larger phytoplankton $> 2 \mu\text{m}$, including diatoms (dominated by increases of large centrics but also including increased rare but toxic *Pseudo-nitzschia*) and large increases of nanoflagellates. Dinoflagellates decreased, such that the community shifted from dinoflagellate to diatom/nanoflagellate-dominance. Among autotrophs, increased N:P may have favoured large diatoms and nanoflagellates with respect to dinoflagellates, while among heterotrophs, increases in bacteria and small ciliates were potentially favoured through N enrichment and food-web processes.

Because the enrichment was expressed not only as changed biomass but also changed community composition, there was potential for reduced nutritional quality of the phytoplankton for higher trophic levels, given the decrease of potentially more nutritious dinoflagellate biomass. The substantial increases of phytoplankton $> 2 \mu\text{m}$ and large centric diatoms in particular indicated potential for enhanced sedimentation of organic matter, possibly explaining decreases

in sediment denitrification recorded between early and late stages of the time series (Zeldis and Swaney 2018) and the source of the DIN increase over the time series.

Seasonality of the primary production cycle and nutrient limitation in the Firth underpin a transition from net-autotrophy in spring to early summer, toward net-heterotrophy in late summer and autumn (Zeldis et al. 2022) with late-season expression of depressed O₂ and pH linked to mineralisation of biomass. The observations made here of increased N and microplankton indicate a continuation of enrichment the Firth has received over decades and support previous conclusions that plankton at the base of the Firth food web are pivotal in the expression of ecosystem stressors (Zeldis and Swaney 2018). Our study thus shows the value of long-term records of microplankton population change, in identifying and explaining important drivers of coastal ecosystem health.

Supplementary Information The online version contains supplementary material available at <https://doi.org/10.1007/s12237-022-01099-1>.

Acknowledgements We thank scientific staff and crews of NIWA R.V.s *Kaharoa*, *Tangaroa* and Western Work Boats *Star Keys* who enabled the ocean-going data, the NIWA Water Quality Laboratory for sample analysis, Jochen Bind for database administration and Scott Nodder for manuscript review. We thank journal reviewers and editors.

Funding Project support was from the New Zealand Ministry of Business, Innovation and Employment (MBIE)-funded ‘Coasts and Oceans’ Outcome-Based Investment contract C01X0501 and NIWA Strategic Science Investment Fund project ‘Ocean Flows and Productivity’ (COOF2202). Funds for open access fees were from ‘Ocean Flows and Productivity’ (COOF2202).

Open Access This article is licensed under a Creative Commons Attribution 4.0 International License, which permits use, sharing, adaptation, distribution and reproduction in any medium or format, as long as you give appropriate credit to the original author(s) and the source, provide a link to the Creative Commons licence, and indicate if changes were made. The images or other third party material in this article are included in the article's Creative Commons licence, unless indicated otherwise in a credit line to the material. If material is not included in the article's Creative Commons licence and your intended use is not permitted by statutory regulation or exceeds the permitted use, you will need to obtain permission directly from the copyright holder. To view a copy of this licence, visit <http://creativecommons.org/licenses/by/4.0/>.

References

- Alexander, T.J., P. Vonlanthen, and O. Seehausen. 2017. Does eutrophication-driven evolution change aquatic ecosystems? *Philosophical Transactions of the Royal Society B: Biological Sciences* 372: 20160041.
- Anderson, D.M., J.M. Burkholder, W.P. Cochlan, P.M. Glibert, C.J. Gobler, C.A. Heil, R.M. Kudela, M.L. Parsons, J.E.J. Rensel, D.W. Townsend, V.L. Trainer, and G.A. Vargo. 2008. Harmful algal blooms and eutrophication: Examining linkages from selected coastal regions of the United States. *Harmful Algae* 8: 39–53.
- Antia, N.J., P.J. Harrison, and L. Oliveira. 1991. The role of dissolved organic nitrogen in phytoplankton nutrition, cell biology and ecology. *Phycologia* 30: 1–89.
- Azam, F., T. Fenchel, J. Field, J.S. Gray, L. Meyer, and T.F. Thingstad. 1983. The ecological role of water-column microbes in the sea. *Marine Ecology Progress Series* 10: 257–263.
- Baird, R.B. 2017. Standard methods for the examination of water and wastewater. 23rd. Water Environment Federation, American Public Health Association, American Water Works Association.
- Berman, T., and D.A. Bronk. 2003. Dissolved organic nitrogen: A dynamic participant in aquatic ecosystems. *Aquatic Microbial Ecology* 31: 279–305.
- Boynton, W., W. Kemp, and C. Keefe. 1982. *A comparative analysis of nutrients and other factors influencing estuarine phytoplankton production*. New York: Academic.
- Boynton, W., and W. Kemp. 2008. Estuaries. In *Nitrogen in the Marine Environment*, ed. D. Capone, D. Bronk, M. Mulholland, and E. Carpenter, 809–856. Burlington, Massachusetts: Elsevier.
- Buitenhuis, E.T., W.K.W. Li, D. Vault, M.W. Lomas, M.R. Landry, F. Partensky, D.M. Karl, O. Ulloa, L. Campbell, S. Jacquet, F. Lantoine, F. Chavez, D. Macias, M. Gosselin, and G.B. McManus. 2012. Picophytoplankton biomass distribution in the global ocean. *Earth Systems Science Data* 4: 37–46.
- Bury, S.J., and J.R., Zeldis, S.D. Nodder, and M. Gall. 2012. Regenerated primary production dominates in a periodically upwelling shelf ecosystem, northeast New Zealand. *Continental Shelf Research* 32: 1–21. <https://doi.org/10.1016/j.csr.2011.09.008>.
- Capriulo, G.M., G. Smith, R. Troy, G.H. Wikfors, J. Pellet, and C. Yarish. 2002. The planktonic food web structure of a temperate zone estuary, and its alteration due to eutrophication. In *Nutrients and Eutrophication in Estuaries and Coastal Waters*, ed. Orive E., Elliott M. and d.J. V.N. Dordrecht: Springer.
- Chan, A.T. 1980. Comparative physiological study of marine diatoms and dinoflagellates in relation to irradiance and cell size. Ii. Relationship between photosynthesis, growth, and carbon/chlorophyll a ratio^{1,2}. *Journal of Phycology* 16: 428–432.
- Chang, F.H., J. Zeldis, M. Gall, and J. Hall. 2003. Seasonal and spatial variation of phytoplankton functional groups on the northeastern New Zealand continental shelf and in Hauraki Gulf. *Journal of Plankton Research* 25: 737–758.
- Chisholm, S.W. 1992. Phytoplankton size. In *Primary Productivity and Biogeochemical Cycles in the Sea*, ed. Falkowski P.G., Woodhead A.D. and V. K. Boston, MA: Environmental Science Research, Springer.
- Christaki, U., S. Jacquet, J.R. Dolan, D. Vault, and F. Rassoulzadegan. 1999. Growth and grazing on *Prochlorococcus* and *Synechococcus* by two marine ciliates. *Limnology and Oceanography* 44: 52–61.
- Cloern, J.E. 2001. Our evolving conceptual model of the coastal eutrophication problem. *Marine Ecology Progress Series* 210: 223–253.
- Cloern, J.E., and A.D. Jassby. 2008. Complex seasonal patterns of primary producers at the land–sea interface. *Ecology Letters* 11: 1294–1303.
- Conley, D.J., J. Carstensen, R. Vaquer-Sunyer, and C.M. Duarte. 2009. Ecosystem thresholds with hypoxia. *Hydrobiologia* 629: 21–29.
- Cook, P.L.M., B.D. Eyre, R. Leeming, and E.C.V. Butler. 2004. Benthic fluxes of nitrogen in the tidal reaches of a turbid, high-nitrate subtropical river. *Estuarine, Coastal and Shelf Science* 59: 675–685.
- Cooper, S.R. 1995. Chesapeake Bay watershed historical land use: Impact on water quality and diatom communities. *Ecological Applications* 5: 703–723.
- Davidson, K., R.J. Gowen, P. Tett, E. Bresnan, P.J. Harrison, A. McKinney, S. Milligan, D.K. Mills, J. Silke, and A.M. Crooks. 2012. Harmful algal blooms: How strong is the evidence that nutrient ratios and forms influence their occurrence? *Estuarine, Coastal and Shelf Science* 115: 399–413.

- Dolan, J.R. 1991. Microphagous ciliates in mesohaline Chesapeake Bay waters: Estimates of growth rates and consumption by copepods. *Marine Biology* 111: 303–309. <https://doi.org/10.1007/BF01319713>
- Duarte, C., S. Agustí, J. Gasol, D. Vaqué, and E. Vázquez-Domínguez. 2000. Effect of nutrient supply on the biomass structure of planktonic communities: An experimental test on a Mediterranean coastal community. *Marine Ecology Progress Series* 206: 87–95.
- Edler, L., and M. Elbrächter. 2010. *The utermöhl method for quantitative phytoplankton analysis*. Paris: UNESCO.
- Edwards, K.F. 2019. Mixotrophy in nanoflagellates across environmental gradients in the ocean. *Proceedings of the National Academy of Sciences* 116: 6211–6220.
- Eppley, R.W., E.H. Renger, and W.G. Harrison. 1979. Nitrate and phytoplankton production in southern California coastal waters. *Limnology and Oceanography* 24: 483–494.
- Eriksen, R.S., C.H. Davies, P. Bonham, F.E. Coman, S. Edgar, F.R. McEnulty, D. McLeod, M.J. Miller, W. Rochester, A. Slotwinski, M.L. Tonks, J. Uribe-Palomino, and A.J. Richardson. 2019. Australia's long-term plankton observations: The integrated marine observing system national reference station network. *Frontiers in Marine Science* 6: 161.
- Eyre, B., and A.P. Ferguson. 2009. Denitrification efficiency for defining critical loads of carbon in shallow coastal ecosystems. *Hydrobiologia* 629: 137–146.
- Falkowski, P.G., A.D. Woodhead, and K. Vivirito. 1992. *Primary Productivity and Biogeochemical Cycles in the Sea*. Boston, MA: Springer.
- Ferreira, J.G., W.J. Wolff, T.C. Simas, and S.B. Bricker. 2005. Does biodiversity of estuarine phytoplankton depend on hydrology? *Ecological Modelling* 187: 513–523.
- Flynn, K.J., A. Mitra, K. Anestis, A.A. Anschütz, A. Calbet, G.D. Ferreira, N. Gypens, P.J. Hansen, U. John, J.L. Martin, J.S. Mansour, M. Maselli, N. Medić, A. Norlin, F. Not, P. Pitta, F. Romano, E. Saiz, L.K. Schneider, W. Stolte, and C. Traboni. 2019. Mixotrophic protists and a new paradigm for marine ecology: Where does plankton research go now? *Journal of Plankton Research* 41: 375–391.
- Fukuda, R., H. Ogawa, T. Nagata, and I. Koike. 1998. Direct determination of carbon and nitrogen contents of natural bacterial assemblages in marine environments. *Applied and Environmental Microbiology* 64: 3352–3358.
- Gall, M., and J. Zeldis. 2011. Phytoplankton biomass and primary production responses to physico-chemical forcing across the northeastern New Zealand continental shelf. *Continental Shelf Research* 31: 1799–1810.
- Glibert, P.M., and M.A. Burford. 2017. Globally changing nutrient loads and harmful algal blooms: Recent advances, new paradigms, and continuing challenges. *Oceanography* 30: 58–69.
- Gobler, C.J., E.L. DePasquale, A.W. Griffith, and H. Baumann. 2014. Hypoxia and acidification have additive and synergistic negative effects on the growth, survival, and metamorphosis of early life stage bivalves. *PLoS ONE* 9: e83648.
- Granéli, E., P. Carlsson, and C. Legrand. 1999. The role of C, N and P in dissolved and particulate organic matter as a nutrient source for phytoplankton growth, including toxic species. *Aquatic Ecology* 33: 17–27.
- Hagy, J., W. Boynton, C. Keefe, and K. Wood. 2004. Hypoxia in Chesapeake Bay, 1950–2001: Long-term change in relation to nutrient loading and river flow. *Estuaries* 27: 634–658.
- Hale, S.S., G. Cicchetti, and C.F. Deacutis. 2016. Eutrophication and hypoxia diminish ecosystem functions of benthic communities in a New England Estuary. *Frontiers in Marine Science* 3: 249.
- Hall, J.A., D.P. Barrett, and M.R. James. 1993. The importance of phytoflagellate, heterotrophic flagellate and ciliate grazing on bacteria and picophytoplankton sized prey in a coastal marine environment. *Journal of Plankton Research* 15: 1075–1086.
- Hall, J.A., K. Safi, M.R. James, J. Zeldis, and M. Weatherhead. 2006. Microbial assemblage during the spring-summer transition on the northeast continental shelf of New Zealand. *New Zealand Journal of Marine and Freshwater Research* 40: 195–210.
- Hansen, B., P.K. Bjornsen, and P.J. Hansen. 1994. The size ratio between planktonic predators and their prey. *Limnology and Oceanography* 39: 395–403.
- Harris, G., G. Batley, D. Fox, D. Hall, P. Jernakoff, R. Molloy, A. Murray, J. Newell, G. Parslow, G. Skyring, and S. Walker. 1996. Port Phillip Bay environmental study final report. CSIRO, Canberra, Australia. 239 pp.
- Hillebrand, H., and C.D., Dürselen, D., Kirschtel, U., Pollinger, and T., Zohary. 1999. Biovolume calculation for pelagic and benthic microalgae. *Journal of Phycology* 35: 403–424.
- Hitchcock, G.L. 1982. A comparative study of the size-dependent organic composition of marine diatoms and dinoflagellates. *Journal of Plankton Research* 4: 363–377.
- Hodgkiss, I.J., and K.C. Ho. 1997. Are changes in N:P ratios in coastal waters the key to increased red tide blooms?, *In Asia-Pacific Conference on Science and Management of Coastal Environment* pp.141–147. Dordrecht: Springer Netherlands.
- Hume, T., P. Gerbeaux, D. Hart, H. Kettles, and D. Neale. 2016. A classification of New Zealand's coastal hydrosystems. NIWA Client Report HAM2016–062. 120 pp. <http://www.mfe.govt.nz/publications/marine/classification-of-new-zealands-coastal-hydrosystems>
- Jowett, I. 2019. Time Trends Software version 6.30 build 14. <http://www.jowettconsulting.co.nz/home/time-1>
- Judd, W. 2015. Natural Values. *New Zealand Geographic* 133: 36–61 May-June 2015.
- Kelly, S., R. Kirikiri, C. Sim-Smith, and S. Lee. 2020. State of our Gulf 2020: Hauraki Gulf/Tīkapa Moana/Te Moana-nui-a-Toi state of the environment report 2020. Auckland. 177 pp. <https://www.aucklandcouncil.govt.nz/about-auckland-council/how-auckland-council-works/harbour-forums/docsstateofgulf/state-gulf-full-report.pdf>
- Kemp, W., P. Sampou, J. Cafrey, M. Mayer, K. Henriksen, and W. Boynton. 1990. Ammonium recycling versus denitrification in Chesapeake Bay sediments. *Limnology and Oceanography* 35: 1545–1563.
- Kemp, W., W.R. Boynton, J.E. Adolphi, D.F. Boesch, W.C. Boicourt, G. Brush, J.C. Cornwell, T.R. Fisher, P.M. Glibert, J.D. Hagy, L.W. Harding, E.D. Houde, D.G. Kimmel, W.D. Miller, R.I.E. Newell, M.R. Roman, E.M. Smith, and J.C. Stevenson. 2005. Eutrophication of Chesapeake Bay: Historical trends and ecological interactions. *Marine Ecology Progress Series* 303: 1–29.
- Krstulović, N., M. Šolić, and I. Marasović. 1998. Relationship between bacteria, phytoplankton and heterotrophic nanoflagellates along the trophic gradient. *Helgoländer Meeresuntersuchungen* 51: 433–443.
- Lachat. 2010. Methods list for automated ion analyzers. http://www.lachatinstrument.com/download/LL022-Methods-List_5-10.pdf
- Law, C.S., J.R. Zeldis, H. Bostock, V. Cummings, K. Currie, G. Frontin-Rollet, H. Macdonald, S. Mikaloff-Fletcher, D. Parsons, N. Ragg, and M. Sewell. 2019. A synthesis of New Zealand ocean acidification research, with relevance to the Hauraki Gulf. NIWA Client Report. 2019165WN.77 pp. <https://waikatoregion.govt.nz/services/publications/tr202016>
- Lin, S., R. Litaker, and W. Sunda. 2015. Phosphorus physiological ecology and molecular mechanisms in marine phytoplankton. *Journal of Phycology* 52: 10–36.
- Mann, K.H., and J.R.N. Lazier. 1991. *Dynamics of marine ecosystems. Biological-physical interactions in the oceans*. Cambridge, Massachusetts: Blackwell Scientific Publications.
- Mastrandrea, M.D., C.B. Field, T.F. Stocker, O. Edenhofer, K.L. Ebi, D.J. Frame, H. Held, E. Kriegler, K.J. Mach, P.R. Matschoss,

- G.-K. Plattner, G.W. Yohe, and F.W. Zwiers. 2010. Guidance Note for Lead Authors of the IPCC Fifth Assessment Report on Consistent Treatment of Uncertainties. Intergovernmental Panel on Climate Change (IPCC) <https://archive.ipcc.ch/pdf/supporting-material/uncertainty-guidance-note.pdf>
- McBride, G.B. 2019. Has water quality improved or been maintained? A quantitative assessment procedure. *Journal of Environmental Quality* 48: 412–420.
- Menden-Deuer, S., and E. Lessard. 2000. Carbon to volume relationships for dinoflagellates, diatoms and other protist plankton. *Limnology and Oceanography* 45: 569–579.
- Monbet, Y. 1992. Control of phytoplankton biomass in estuaries: A comparative analysis of microtidal and macrotidal estuaries. *Estuaries* 15: 563–571.
- Montagnes, D.J.S., and M. Franklin. 2001. Effect of temperature on diatom volume, growth rate, and carbon and nitrogen content: Reconsidering some paradigms. *Limnology and Oceanography* 46: 2008–2018.
- Monger, B.C., and M.R. Landry. 1991. Prey-size dependency of grazing by free-living marine flagellates. *Marine Ecology Progress Series* 74: 239–248.
- NRC. 2000. *Clean Coastal Waters understanding and reducing the effects of nutrient pollution*. Washington DC: National Academy Press.
- Olenina, I., S. Hajdu, L. Edler, A. Andersson, N. Wasmund, S. Busch, J. Göbel, S. Gromisz, S. Huseby, M. Huttunen, A. Jaanus, P. Kokkonen, I. Ledaine, and E. Niemkiewicz. 2006. Biovolumes and size-classes of phytoplankton in the Baltic Sea. HELCOM Baltic Sea Environmental Proceedings. 144.
- Paerl, H.W. 2006. Assessing and managing nutrient-enhanced eutrophication in estuarine and coastal waters: Interactive effects of human and climatic perturbations. *Ecological Engineering* 26: 40–54.
- Parsons, M., Q. Dortch, and R. Turner. 2002. Sedimentological evidence of an increase in *Pseudo-nitzschia* (Bacillariophyceae) abundance in response to coastal eutrophication. *Limnology and Oceanography* 47: 551–558.
- Pearl, R. 2016. *The Story of the Hauraki Gulf: Discovery, Transformation, Restoration*. Auckland: David Bateman Limited.
- Philippart, C.J., G.C. Cadée, W. van Raaphorst, and R. Riegman. 2000. Long-term phytoplankton-nutrient interactions in a shallow coastal sea: Algal community structure, nutrient budgets, and denitrification potential. *Limnology and Oceanography* 45: 131–144.
- Putt, M., and D.K. Stoecker. 1989. An experimentally determined carbon : Volume ratio for marine “oligotrichous” ciliates from estuarine and coastal waters. *Limnology and Oceanography* 34: 1097–1103.
- Rabalais, N.N., R.E. Turner, R.J. Diaz, and D. Justic. 2009. Global change and eutrophication of coastal waters. *ICES Journal of Marine Science* 66: 1528–1537.
- Ragueneau, O., E. De Blas Varela, P. Treguer, B. Queguiner, and Y. Del Amo. 1994. Phytoplankton dynamics in relation to the biogeochemical cycle of silicon in a coastal ecosystem of western Europe. *Marine Ecology Progress Series* 106: 157–172.
- Rassoulzadegan, F., M. Laval-Pento, and R.W. Sheldon. 1988. Partitioning of the food ration of marine ciliates between pico- and nanoplankton. *Hydrobiologia* 159: 75–88.
- Redfield, A.C., B.H. Ketchum, and F.A. Richards. 1963. The influence of organisms on the composition of seawater. In *The Sea*, ed. M.N. Hill, 26–77. New York: Wiley & Sons.
- Rey, C., R. Harris, X. Irigoien, R. Head, and F. Carlotti. 2001. Influence of algal diet on growth and ingestion of *Calanus helgolandicus* nauplii. *Marine Ecology Progress Series* 216: 151–165.
- Reynolds, C.S. 2006. Nutrient uptake and assimilation in phytoplankton. In *The Ecology of Phytoplankton*, ed. C.S. Reynolds, 145–177. Cambridge: Cambridge University Press.
- Rhodes, L., W. Jiang, B. Knight, J. Adamson, K. Smith, V. Langi, and M. Edgar. 2013. The genus *Pseudo-nitzschia* (Bacillariophyceae) in New Zealand: Analysis of the last decade’s monitoring data. *New Zealand Journal of Marine and Freshwater Research* 47: 490–503.
- Riemann, B., H. Havskum, F. Thingstad, and C. Bernard. 1995. The role of mixotrophy in pelagic environments, 87–114. Berlin, Heidelberg: Springer Berlin Heidelberg.
- Safi, K.A., and J.A. Hall. 1999. Mixotrophic and heterotrophic nanoflagellate grazing in the convergence zone east of New Zealand. *Aquatic Microbial Ecology* 20: 83–93.
- Samuelsson, K., and A. Andersson. 2003. Predation limitation in the pelagic microbial food web in an oligotrophic aquatic system. *Aquatic Microbial Ecology* 30: 239–250.
- Sanderson, M.P., D.A. Bronk, J.C. Nejtgaard, P.G. Verity, A.F. Sazhin, and M.E. Frischer. 2008. Phytoplankton and bacterial uptake of inorganic and organic nitrogen during an induced bloom of *Phaeocystis pouchetii*. *Aquatic Microbial Ecology* 51: 153–168.
- Sarthou, G., K.R. Timmermans, S. Blain, and P. Tréguer. 2005. Growth physiology and fate of diatoms in the ocean: A review. *Journal of Sea Research* 53: 25–42.
- Schlitzer, R. 2013. Ocean Data View. <http://odv.awi.de>
- Scully, M.E. 2016. The contribution of physical processes to inter-annual variations of hypoxia in Chesapeake Bay: A 30-yr modeling study. *Limnology and Oceanography* 61: 2243–2260.
- Seitzinger, S., R. Sanders, and R. Styles. 2002. Bioavailability of DON from natural and anthropogenic sources to estuarine plankton. *Limnology and Oceanography* 47: 353–366.
- Shen, C., J.M. Testa, M. Li, W.-J. Cai, G.G. Waldbusser, W. Ni, W.M. Kemp, J. Cornwell, B. Chen, J. Brodeur, and J. Su. 2019. Controls on carbonate system dynamics in a coastal plain estuary: a modeling study. *Journal of Geophysical Research: Biogeosciences* 124.
- Smayda, T.J. 1990. *Novel and nuisance phytoplankton blooms in the sea: evidence for a global epidemic* New York: Elsevier.
- Smayda, T.J. 1997. Harmful algal blooms: Their ecophysiology and general relevance to phytoplankton blooms in the sea. *Limnology and Oceanography* 42: 1137–1153.
- Snelder, T.H., S.T. Larned, and R.W. McDowell. 2018. Anthropogenic increases of catchment nitrogen and phosphorus loads in New Zealand. *New Zealand Journal of Marine and Freshwater Research* 52: 336–361.
- Stoecker, D.K., P.J. Hansen, D.A. Caron, and A. Mitra. 2017. Mixotrophy in the Marine Plankton. *Annual Review of Marine Science* 9: 311–335.
- Stolte, W., and R. Riegman. 1995. Effect of phytoplankton cell size on transient-state nitrate and ammonium uptake kinetics. *Microbiology* 141: 1221–1229.
- Strathman, P. 1967. Estimating the organic carbon content of phytoplankton from cell volume or plasma volume. *Limnology and Oceanography* 12: 411–488.
- Sun, J., and D. Liu. 2003. Geometric models for calculating cell biovolume and surface area for phytoplankton. *Journal of Plankton Research* 25: 1331–1346.
- Sunda, W., and W.-J. Cai. 2012. Eutrophication induced CO₂-acidification of subsurface Coastal Waters: Interactive effects of temperature, salinity and atmospheric pCO₂. *Environmental Science and Technology* 46: 10651–10659.
- Sutula, M. 2011. Review of indicators for development of nutrient numeric endpoints in California estuaries. Southern California Coastal Water Research Project Technical Report. 269.

- Tait, L.W., A.M. Lohrer, M. Townsend, J. Atalah, O. Floerl, and G.J. Inglis. 2020. Invasive ecosystem engineers threaten benthic nitrogen cycling by altering native infaunal and biofouling communities. *Scientific Reports* 10: 1581.
- Tilman, D. 1977. Resource competition between plankton algae: An experimental and theoretical approach. *Ecology* 58: 338–348.
- Turner, R., and N. Rabalais. 1991. Changes in Mississippi River water quality this century: Implications for coastal food webs. *BioScience* 41: 140–147.
- Unrein, F., R. Massana, L. Alonso-Sáez, and J.M. Gasol. 2007. Significant year-round effect of small mixotrophic flagellates on bacterioplankton in an oligotrophic coastal system. *Limnology and Oceanography* 52: 456–469.
- Uye, K., and K. Sano. 1998. Seasonal variations in biomass, growth rate and production rate of the small cyclopoid copepod *Oithona davisae* in a temperate eutrophic inlet. *Marine Ecology Progress Series* 163: 37–44.
- Vant, B. 2013. Trends in river water quality in the Waikato region, 1993–2012. *Waikato Regional Council Technical Report*. 2013 (20): 50.
- Wallace, R.B., H. Baumann, J.S. Grear, R.C. Aller, and C.J. Gobler. 2014. Coastal ocean acidification: The other eutrophication problem. *Estuarine, Coastal and Shelf Science* 148: 1–13.
- Wood, S.N. 2006. *Generalized additive models: an introduction with R*: Chapman and Hall/CRC.
- Wood, S.N. 2011. Fast stable restricted maximum likelihood and marginal likelihood estimation of semiparametric generalized linear models. *Journal of the Royal Statistical Society: Series B (statistical Methodology)* 73: 3–36.
- Worden, A.Z., J.K. Nolan, and B. Palenik. 2004. Assessing the dynamics and ecology of marine picophytoplankton: The importance of the eukaryotic component. *Limnology and Oceanography* 49: 168–179.
- Zeldis, J.R., and R.I.C.C. Francis. 1998. A daily egg production method estimate of snapper biomass in Hauraki Gulf, New Zealand. *ICES Journal of Marine Science: Journal Du Conseil* 55: 522–534.
- Zeldis, J., M.R. James, J. Grieve, and L. Richards. 2002. Omnivory by copepods in the New Zealand subtropical frontal zone. *Journal of Plankton Research* 24: 9–23.
- Zeldis, J.R., J. Oldman, S.L. Ballara, and L.A. Richards. 2005. Physical fluxes, pelagic ecosystem structure, and larval fish survival in Hauraki Gulf, New Zealand. *Canadian Journal of Fisheries and Aquatic Sciences* 62: 593–610.
- Zeldis, J.R., and K.J. Willis. 2015. Biogeographic and trophic drivers of mesozooplankton distribution on the northeast continental shelf and in Hauraki Gulf, New Zealand. *New Zealand Journal of Marine and Freshwater Research* 49: 69–86.
- Zeldis, J.R., and D.P. Swaney. 2018. Balance of catchment and offshore nutrient loading and biogeochemical response in four New Zealand coastal systems: Implications for resource management. *Estuaries and Coasts* 41: 2240–2259.
- Zeldis, J.R., and M. Décima. 2020. Mesozooplankton connect the microbial food web to higher trophic levels and vertical export in the New Zealand Subtropical Convergence Zone. *Deep Sea Research Part I: Oceanographic Research Papers* 155: 103146.
- Zeldis, J.R., K.I. Currie, S.L. Graham, and M.P. Gall. 2022. Attributing controlling factors of acidification and hypoxia in a deep, nutrient-enriched estuarine embayment. *Frontiers in Marine Science* 8: 2107.
- Zhou, F., F. Chai, D. Huang, M. Wells, X. Ma, Q. Meng, H. Xue, J. Xuan, P. Wang, X. Ni, Q. Zhao, C. Liu, J. Su, and H. Li. 2020. Coupling and decoupling of high biomass phytoplankton production and hypoxia in a highly dynamic coastal system: The Changjiang (Yangtze River) estuary. *Frontiers in Marine Science* 7: 259.